TECHNICAL REPORT STANDARD TITLE PAGE

1. Report No. FHWA/TX-87+401-7	2. Government Accession No.	3. Recipient's Catalog No.
4. Title and Subtitle EFFECT OF PRESTRESS ON THE FATIGUE LIFE OF CONCRETE		5. Report Date November 1986
		6. Performing Organization Code
7. Author(s) Way Seng Chia, Ned H. Burns, and B. Frank McCullough		8. Performing Organization Report No. Research Report 401-7
9. Performing Organization Name and Address Center for Transportation Research The University of Texas at Austin Austin, Texas 78712-1075		10. Work Unit No.
		11. Contract or Grant No. Research Study 3-8-84-401
12. Sponsoring Agency Name and Address Texas State Department of Highways and Public Transportation; Transportation Planning Division P. O. Box 5051 Austin, Texas 78763-5051		13. Type of Report and Period Covered Interim
		14. Sponsoring Agency Code

15. Supplementary Notes

Study conducted in cooperation with the U. S. Department of Transportation, Federal Highway Administration. Research Study Title: "Prestressed Concrete Pavement Design—Design and Construction of Overlay Applications"

16. Abstract

This report presents results of a series of regression analyses carried out on data from both the Portland Cement Association and The University of Texas at Austin's test program on fatigue of prestressed concrete beams.

Among the topics investigated were (1) the effect of prestress on the fatigue life of concrete, (2) the interaction of the static stresses due to prestressing and the dynamic stresses due to vehicular loadings, (3) the effect of prestress in delaying micro-crack propagation in concrete, and (4) the effect of prestress on the elasto-plastic behavior of prestressed concrete.

As a result of this investigation, some salient facts about current fatigue design considerations for prestressed concrete pavement seem to emerge.

(1) Present fatigue design is too conservative because it does not consider the beneficial effect of prestressing in helping to delay crack propagation.

(2) For prestress levels of 300 psi or less, the current fatigue design is conservative because the fatigue life of the prestressed specimens was higher than the fatigue life of plain concrete. However, there is a strong indication that this may not be true with prestress levels higher than 300 psi.

(3) The current design method of using superposition of stresses may not be valid because the fatigue life is dependent on the interaction between the static and dynamic stresses due to the prestressing and vehicular loading, respectively.

(4) Prestressing helps in maintaining elasto-plastic behavior, which is ignored in current fatigue design.

17. Key Words regression analysis, fatigue life, prestressed concrete beams, prestress levels, microcracks, literature review, PCA study	18. Distribution Statement No restrictions. This document is available to the public through the National Technical Information Service, Springfield, Virginia 22161.

19. Security Classif. (of this report)	20. Security Classif. (of this page)	21. No. of Pages	22. Price
Unclassified	Unclassified	130	

Form DOT F 1700.7 (8-69)

EFFECT OF PRESTRESS ON THE FATIGUE LIFE OF CONCRETE

by

Way Seng Chia
Ned H. Burns
B. Frank McCullough

Research Report 401-7

Prestressed Concrete Pavement Design-
Design and Construction of Overlay Applications
Research Project 3-8-84-401

conducted for

Texas State Department of Highways
and Public Transportation

in cooperation with the
U.S. Department of Transportation
Federal Highway Administration

by the

Center for Transportation Research
Bureau of Engineering Research
The University of Texas at Austin

November 1986

PREFACE

This is the seventh report in the series describing the research work accomplished on Research Project 3-8-84-401, "Prestressed Concrete Pavement Design - Design and Construction of Overlay Applications."

This report deals with the investigation of current fatigue design of prestressed concrete pavements. Topics discussed in this report include the effect of prestress on the fatigue life of concrete, the effect of prestress on the structural stiffness of the prestressed concrete pavement after bottom cracking, and the interaction between the static stresses due to prestressing and the dynamic stresses due to vehicular loading.

The authors gratefully acknowledge the contributions from Alberto Mendoza-Diaz, Brian W. Dunn, and Joe Maffei, fellow graduate students working on the same project. Appreciation and thanks are also extended to the staff of the Center for Transportation Research, especially to Lyn Gabbert and Rachel Hinshaw, for putting this report together. The authors are also very grateful to Rouault Ray Buvia whose assistance in the electronic instrumentation was essential in conducting this research.

Way Seng Chia
Ned H. Burns
B. Frank McCullough

LIST OF REPORTS

Report No. 401-1, "Very Early Post-tensioning of Prestressed Concrete Pavements," by J. Scott O'Brien, Ned H. Burns and B. Frank McCullough, presents the results of tests performed to determine the very early post-tensioning capacity of prestressed concrete pavement slabs, and gives recommendations for a post-tensioning schedule within the first 24 hours after casting.

Report No. 401-2, "New Concepts in Prestressed Concrete Pavement," by Neil D. Cable, Ned H. Burns, and B. Frank McCullough, presents the following: (a) a review of the available literature to ascertain the current state of the art of prestressed concrete pavement; (b) a critical evaluation of the design, construction, and performance of several FHWA sponsored prestressed concrete pavement projects which were constructed during the 1970s; and (c) several new prestressed concrete pavement concepts which were developed based on (a) and (b).

Report No. 401-3, "Behavior of Long Prestressed Pavement Slabs and Design Methodology," by Alberto Mendoza-Diaz, N. H. Burns, and B. Frank McCullough, presents the development of a model to predict the behavior of long prestressed concrete pavement (PCP) slabs and incorporate the predictions from the model into a design procedure.

Report No. 401-4, "Instrumentation and Behavior of Prestressed Concrete Pavements," by Joseph R. Maffei, Ned H. Burns, and B. Frank McCullough, describes the development and implementation of an instrumentation program used to monitor the behavior of a one-mile-long experimental prestressed concrete pavement and presents the results of measurements of ambient and concrete temperatures, horizontal slab movement, slab curling, concrete strain, very early concrete strength, concrete modulus of elasticity, and slab cracking.

Report No. 401-5, "Field Evaluation of Subbase Friction Characteristics," by Way Seng Chia, Ned H. Burns, and B. Frank McCullough, presents the results of push-off tests performed on four experimental test slabs at Valley View, Texas, to determine the maximum coefficient of friction of several friction reducing mediums for future implementation in the prestressed pavement projects in Cooke and McLennan counties.

Research Report No. 401-6, "Friction Losses in Unbonded Post-Tensioning Tendons," by Brian W. Dunn, Ned H. Burns, and B. Frank McCullough, presents results from experimental tests at Valley View, Texas, to determine friction losses in post-tensioning tendons to be used in the prestressed concrete pavement project in McLennan county, Texas. Collected data from the pavement project are also presented.

Research Report No. 401-7, "Effect of Prestress on the Fatigue Life of Concrete," by Way Seng Chia, Ned H. Burns, and B. Frank McCullough, presents results from fatigue tests on prestressed concrete beams conducted at the Portland Cement Association and The University of Texas at Austin to determine the effects of prestressing on the fatigue life of concrete.

ABSTRACT

Currently, there are some underlying assumptions made in the fatigue design of prestressed concrete pavements that may be too conservative or sometimes unconservative. These assumptions are:

(1) Prestressing does not help in any way to delay crack propagation in concrete. Therefore, fatigue design is usually based on the fatigue life of plain concrete.

(2) The principle of superposition of stresses is used to obtain the resultant stress at the bottom surface of the prestressed pavement. Therefore, the difference between the static nature of prestress and the dynamic nature of vehicular stresses is not accounted for.

(3) Prestressed concrete pavements behave like unreinforced or reinforced concrete pavements. The ability of prestressed concrete pavement to exhibit elasto-plastic behavior is ignored.

This report presents an investigation into the validity of those assumptions. Regression analysis on data from both the Portland Cement Association and The University of Texas at Austin test programs resulted in these conclusions:

(1) Prestressing helps to delay propagation of microcracks in concrete.

(2) An increase in the amount of prestress will increase the absolute value of the slopes of the equations representing the relationship between stress levels and the logarithm of number of cycles at failure.

(3) The fatigue strength at 10 million cycles decreases with an increase in the level of prestress. However, specimens having prestress levels of 50 to 300 psi still have a higher fatigue strength than plain concrete.

(4) The assumption of superposition of stresses is not valid because the fatigue life of prestressed concrete is dependent on the interaction of the static nature of prestress and the dynamic nature of the vehicular stresses.

(5) The structural integrity of the fatigue test specimens is highly dependent on the amount of prestress. Specimens subjected to higher prestress level were able to maintain better elasto-plastic behavior.

SUMMARY

This report presents results of a series of regression analyses carried out on data from both the Portland Cement Association and The University of Texas at Austin's test program on fatigue of prestressed concrete beams.

Among the topics investigated were (1) the effect of prestress on the fatigue life of concrete, (2) the interaction of the static stresses due to prestressing and the dynamic stresses due to vehicular loadings, (3) the effect of prestress in delaying micro-crack propagation in concrete, and (4) the effect of prestress on the elasto-plastic behavior of prestressed concrete.

As a result of this investigation, some salient facts about current fatigue design considerations for prestressed concrete pavement seem to emerge.

(1) Present fatigue design is too conservative because it does not consider the beneficial effect of prestressing in helping to delay crack propagation.

(2) For prestress levels of 300 psi or less, the current fatigue design is conservative because the fatigue life of the prestressed specimens was higher than the fatigue life of plain concrete. However, there is a strong indication that this may not be true with prestress levels higher than 300 psi.

(3) The current design method of using superposition of stresses may not be valid because the fatigue life is dependent on the interaction between the static and dynamic stresses due to the prestressing and vehicular loading, respectively.

(4) Prestressing helps in maintaining elasto-plastic behavior, which is ignored in current fatigue design.

IMPLEMENTATION STATEMENT

This report presents the results of the regression analysis carried out on data from both the Portland Cement Association and The University of Texas test programs on fatigue of prestressed concrete. Although more research is still needed, the results of the regression analysis may be used to modify or refine the PCP1 program for designing prestressed concrete pavement. An important criterion that should be incorporated into the fatigue design of prestressed concrete is the effect different levels of prestress have on the fatigue life of concrete.

TABLE OF CONTENTS

CHAPTER 1. INTRODUCTION

BACKGROUND

Prestressed pavements are slabs that have been precompressed by the application of a permanent compressive force in order to increase their capacity to withstand flexural stresses developed by highway vehicles (Ref 1).

An important consideration in the design of prestressed concrete pavements is the amount of permanent pre-compressive force to be applied to the slabs. Since the compressive strength of concrete is high compared to its flexural strength, there is a wide range of prestress levels from which to choose.

This is especially evident if we consider prestressed pavements on a worldwide scale. The highest pre-compressive stress applied was found to be the 1,138 psi in a pavement constructed in 1958 in Anif-Saltzburg, Austria. The lowest was the 90 psi in a highway constructed in 1951 in Wexham Springs, Buckinghamshire, Great Britian (Ref 2).

A survey of the prestressed concrete pavements built in the United States in the last 15 years is shown in Table 1.1. The average pavement thickness was found to be 6 inches, with slab length varying from 300 feet to 760 feet long. The prestress level applied ranged from 200 psi to 331 psi (Refs 1, 2, 3, and 4).

Currently the amount of prestress to be applied is governed by two main considerations:

(1) The thickness of the pavement. Since prestressed pavement are usually thinner, higher wheel load stresses are developed at the base.

(2) The longer slab lengths used in prestressed pavements. They produce higher frictional resistance during low temperature cycles, resulting in higher tensile stresses in the concrete as a result of slab shortening.

The amount of pre-compressive stress applied must at least be sufficient to compensate for the increase in flexural/tensile stresses.

TABLE 1.1. PRESTRESSED CONCRETE DEMONSTRATION PROJECT IN THE UNITED STATES

		Pavement Dimensions			Prestress (psi)	
Date	Location	Length (feet)	Width (feet)	Thickness (feet)	Longitudinal	Transverse
1971	Milford, Delaware	300	14	6	238	None
1971	Dulles International Airport, Virginia	400 500 600 760 500 400	24	6	200	None
1973	Harrisburg, Pennsylvania	600	24	6	331	None
1973	Kutztown, Pennsylvania	500	24	6	331	None
1977	Tempe, Arizona	400	24	6	215	None
1978	Brookhaven, Mississippi	400	24	6	229	None

FATIGUE DESIGN ASPECT OF PRESTRESSED PAVEMENT

The current fatigue design for prestressed concrete pavement includes only the flexural/tensile stress aspect. That is, the net flexural/tensile stress at the base at the midspan of the slab is determined using the equation

$$f_n = f_r + f_p \pm f_t - f_f - f_l$$

where

f_n	=	net flexural stress at midslab,
f_r	=	flexural strength of concrete,
f_p	=	compressive stress due to prestress,
f_t	=	stress due to temperature and moisture gradient,
f_f	=	restraint stress due to subbase friction, and
f_l	=	stress due to wheel load.

The reason why the (+) and (-) signs are used to account for f_t is that with a drop in temperature tensile stresses are induced at the base, while with a rise in temperature compressive stresses are induced at the base. Based on the ratio of f_n/f_r, the fatigue life of the pavement can be determined using equations derived from the AASHTO field survey of reinforced concrete pavements or through experimental work done on the flexural fatigue of plain concrete. The actual fatigue design is much more complicated because of the changing environmental and loading conditions and involves the application of Miner's hypothesis. More comprehensive procedure for designing prestressed pavements by flexural fatigue can be found in both Refs 5 and 12.

An important aspect that has been ignored is the effect of the prestress on the fatigue life of the concrete, i.e., how different levels of prestress affect the fatigue life of the concrete.

It must also be mentioned that the compressive stress due to external prestress is static in nature, whereas the flexural stress due to the wheel load is dynamic in nature. The stresses due to temperature, moisture gradient, and restraint of movement due to subbase friction are dependent on the time of day and the temperature.

Current fatigue design consideration for prestressed pavement uses the principle of superposition of this stress without considering the static and dynamic nature of the loading conditions. This raises several questions. Is this practice fundamentally correct and is it conservative? What is the relationship between the static stresses due to prestressing and the dynamic stresses due to wheel loading? How does this relationship affect fatigue design for prestressed concrete pavements? These are important questions for which no answers are available as yet.

RESEARCH ON FATIGUE OF CONCRETE

Two approaches are usually associated with fatigue research on concrete: fundamental and phenomenological. While fundamental studies are made to enhance the knowledge of the behavior of concrete, phenomenological studies are directed toward practical applications of concrete (Ref 6).

While several studies have been done on flexural fatigue of plain concrete, very few studies have been carried out to determine the effect of prestress on the fatigue life of concrete. This knowledge will be especially helpful in fatigue design of prestressed concrete pavement where serviceability failures are usually determined by the amount of cracking of the concrete. This is because, unlike the design of prestressed bridge slabs, the primary purpose of the prestressing strands is to apply a longitudinal compressive force on the slab and not to carry the flexural stresses caused by the wheel load. That is why the prestressing strands are usually located at the mid-depth of the slabs and are not draped.

This report presents a laboratory investigation into the phenomenological effect of different levels of low prestress (10 percent to 50 percent of the flexural strength of concrete) on the fatigue life of concrete.

This research was prompted by fundamental studies conducted on microcracking of concrete at Cornell University by Sturman, Shah, and Winters (Ref 7), and also by research work done on reinforced and prestressed concrete pavements constructed with expansive concrete (Ref 8).

Microscopic and X-ray studies at Cornell showed that bond cracks (between coarse aggregates and mortar) exist in plain concrete to a sizeable degree before the concrete is subjected to any external loading. It was found that these bond cracks were caused by tensile stresses due to volume changes during hydration, temperature changes, and mortar settlement. The fact that significant random bond cracks exist in hardened concrete prior to loading explains the low tensile strength of concrete. The disintegration of concrete when subjected to cyclic loading is due to the propagation of these microcracks.

There is currently very little information available on how a small externally applied compressive force will affect the propagation of these microcracks when concrete is subjected to flexural cyclic loading. However, it is conjectured that a small compressive force may help to delay the propagation of these microcracks. Supporting evidence can be found in studies of continuously reinforced and prestressed concrete pavements made with expansive cement. It was found that compressive stress in the concrete was as much as 300 psi during the early curing period. Although this compressive stress dropped to 150 psi in the latter stages, it was found that the induced compressive stresses help to reduce cracking in the concrete pavements. The use of expansive cement has the effect of delaying the time when contraction occurs and allows the concrete to gain significantly in strength before it goes into tension.

Also, a re-examination of the data from some prestressed beam tests conducted by the Portland Cement Association shows a strong indication that a small compressive stress may indeed increase the fatigue life of concrete (Ref 9). The details of this study are discussed in the introduction to Chapter 3.

OBJECTIVES AND SCOPE

In an effort to come up with more useful applications of prestressed pavement, research was undertaken at The University of Texas at Austin to look into new design methods for prestressed concrete pavement for overlay purposes and to monitor its performance. This study was sponsored by the Texas State Department of Highways and Public Transportation (SDHPT) and the Federal Highway Administration. The overall scope of the study includes making new design recommendations, determining new ways of stressing the prestressing tendons, monitoring the prestressed pavement over seasonal changes, and evaluating the performance of the transverse joints.

As part of this project, a limited laboratory investigation was carried out to determine what effect different levels of prestress have on the fatigue life of concrete. This report presents only the results of that study and the re-evaluation of a previous series of tests by the Portland Cement Association. For results of the other studies, readers are referred to References 10 to 14.

Specifically, the objectives of this study are

(1) to determine the effect of different levels of prestress on the fatigue life of concrete,

(2) to compare the fatigue life of prestressed concrete with the fatigue life of plain concrete and to determine whether current fatigue design consideration based on the fatigue life of plain concrete is conservative,

(3) to determine whether prestressing helps to delay the propagation of micro-cracks,

(4) to study the interaction between the static stresses due to prestressing and dynamic stresses due to wheel loading, and

(5) to study the effect of prestress on the flexural stiffness of prestressed concrete after the first crack.

REVIEW OF CHAPTERS

Chapter 2 presents a literature review of previous studies on flexural fatigue of plain concrete. Important parameters used to present fatigue life of plain concrete that are investigated include range of stress, rest periods, endurance limit, speed of testing, cumulative fatigue damage according to Miner's Hypothesis, modified Goodman diagram, and probability concepts.

Chapter 3 presents the re-examination of a previous study on the effect of prestress on fatigue life of concrete conducted by the Portland Cement Association. Also included are the experimental testing of prestressed concrete beams carried out at The University of Texas at Austin.

Chapter 4 presents the data from an earlier study conducted by the Portland Cement Association and the data collected in this study. The analysis of these data is carried out in Chapter 5.

The final chapter presents the conclusions of this study and recommendations for further research in this area.

CHAPTER 2. FLEXURAL FATIGUE OF PLAIN CONCRETE

Due to the nature of vehicular loadings, concrete pavements are subjected to repeated loadings of varying magnitudes. Under these repeated loading conditions, the strength of the concrete is reduced and the concrete may fail at a strength much lower than its static strength. This phenomenon is called fatigue failure.

Microcracks exist in concrete to a sizeable degree before the concrete is even subjected to any external loading. These microcracks are bond cracks caused by tensile stresses due to volume changes during hydration, temperature changes, and mortar settlement. These microcracks act as stress raisers and propagation of these microcracks depends on the rate at which the energy provided by the vehicular loadings is absorbed. The energy absorption rate is related to the size of the hysteresis loop on each cycle of applied load. This is in turn related to the range of the applied stress the concrete pavement is subjected to. A larger variation in tensile stress is produced at the base of the pavement due to a heavy truck than due to a passenger car. Therefore more damage is done by each passing truck than by a passenger car. These damages are cumulative and ultimately these microcracks will propagate to the surface, leading to major surface cracking and serviceability failure (Ref 15).

EARLY RESEARCH ON FLEXURAL FATIGUE

The problem of flexural fatigue was first investigated in the early 1920's by Clemmer of the Illinois Department of Highways (Ref 16). His study on corner failures of concrete pavement slabs led him to believe that these failures were due to repeated wheel loads. He reasoned that the corners behaved as cantilever beams and he devised an ingenious testing device consisting of seven specimens cantilevered from a central hub, much like spokes of a wheel. The loads were applied through a truck wheel and axle which traveled a circular track about a fixed vertical shaft (Ref 15).

Concurrently at Purdue University, Hatt and Crepps were testing plain concrete specimens under completely reversed fatigue loading (Ref 17). To more closely simulate the vehicular conditions, Hatt argued that the frequency in the Illinois test (40 cpm) was too great and tested his specimens at 10 cpm. Hatt's specimens were also subjected to overnight and weekend rest periods.

The results of these early tests are not presented here as the authors feel that no significant benefit can be derived from repeating what has been so excellently presented by Murdock (Ref 15) and Nordby (Ref 18). Although the results of these early test have been superseded by more extensive studies carried out in the 50's and 60's, their significant contributions in laying the groundwork for future research cannot be overemphasized. What is presented, however, is the current state of knowledge of flexural fatigue, which is relevant to our fatigue testing of prestressed concrete beams. The important topics considered are fatigue limit, range of loading stresses, modified Goodman diagram, reversal of loading, effect of rest periods, effect of rate of loading, probability concept in fatigue, and Miner's Hypothesis.

CURRENT STATE OF KNOWLEDGE

The summaries presented are from flexural tests conducted from the 1920's to the early 1970's. For the past 15 years, very few extensive studies have been done on flexural fatigue of plain concrete.

In order to obtain useful fatigue test results, the tests have to be conducted on groups of identical specimens. Since concrete is a non-homogeneous material, it is practically impossible to fabricate concrete specimens which are identical. Therefore, concrete fatigue data are usually normalized, i.e., the maximum applied stress is divided by the beam's modulus of rupture. This ratio is known as the stress ratio or stress level. The beam's modulus of rupture can be determined by static tests either on companion specimens or on broken "halves" of failed fatigue specimens. Either a 1/3 point or center point loading method can be used for this purpose. Although considerable scatter is observed in modulus of rupture data, the 1/3 point loading will give slightly lower values than with center point loading.

The general relationship of stress ratio versus number of cycles to failure is usually presented as an S-N curve, as shown in Fig 2.1.

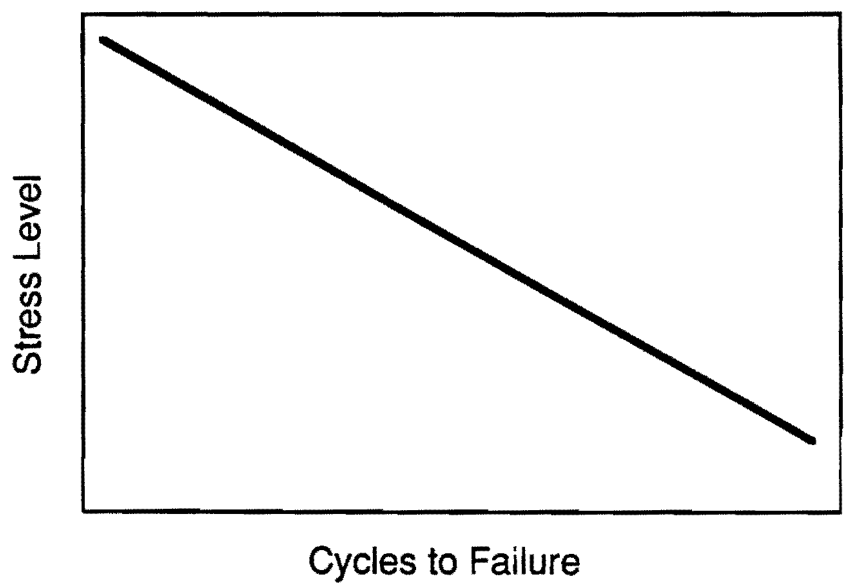

Fig 2.1. Typical S-N curve for fatigue of concrete.

Fatigue Limit

Fatigue limit is defined as the stress level at which concrete can withstand an infinite number of cycles without cracking (failure). This means that the ordinate at that stress level will become asymptotic to the horizontal axis. This is shown graphically in Fig 2.2.

Clemmer was the first to suggest that a fatigue limit might exist for plain concrete. When Clemmer subjected his specimens to stresses of 48 percent of the sample's flexural strength (a stress level of 0.48), he found that all these specimens were able to endure 2,000,000 cycles without failure. The stress level was then increased to 0.54. Most of the specimen failed with less than 700,000 additional cycles. However, a few specimens were able to withstand a cumulative applications of 3,000,000 cycles without failure. From the results of his tests, Clemmer suggested that the fatigue limit of concrete in flexure is between 51 and 54 percent of its static strength.

The existence of a fatigue limit was further corroborated by tests carried out by Hatt and Crepps at Purdue University. In the Purdue tests, age of specimens was an added variable. Results of these tests indicate that the fatigue limit for mortar specimens over 6 months old was between 54 and 55 percent of the sample's flexural strength and between 50 and 55 percent for 4–month–old specimens. No fatigue limit was established for the 28-day specimens.

Currently, the belief is that no flexural fatigue limit exists for concrete. This came about as a result of extensive studies conducted by Kesler at the University of Illinois (Ref 6). Kesler found that the line representing the fatigue strength continues to slope downwards even at the 10,000,000 cycles limit. This led most researchers to describe fatigue behavior by using the term "fatigue strength". The term fatigue strength is always used in relationship to a fixed number of cycles of loading. For example, Kesler found that the fatigue strength of plain concrete subjected to 10,000,000 cycles of repeated flexural loadings is about 55 percent of its static ultimate flexural strength.

Range of Loading Stress

It must be pointed out that the fatigue limit of Clemmer's tests and the fatigue strength of Kesler's tests were determined from tests on specimens where the minimum stress was

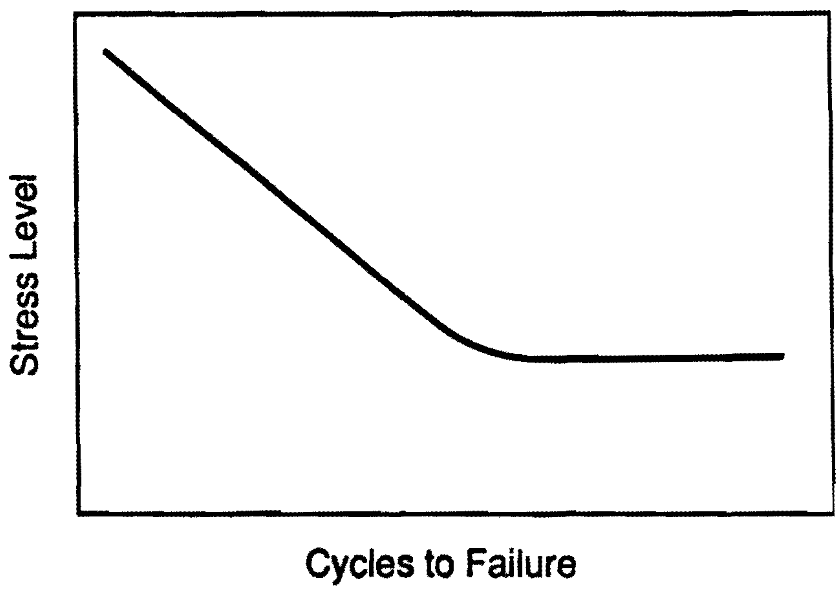

Fig 2.2. S-N curve with a fatigue limit.

kept constant at zero. The fatigue limits suggested by Hatt and Crepps were from tests conducted on specimens subjected to reversed fatigue loading.

Tests conducted by Murdock and Kesler have shown that the range of stresses the specimens are subjected to has a profound effect on the fatigue strength of concrete (Ref 15). For easier understanding, the terminologies and notation used in Murdock and Kesler's tests are explained below:

f_1	=	flexural stress at minimum load,
f_2	=	flexural stress at maximum load,
f_r	=	modulus of rupture as determined from static tests of broken "halves" of failed specimens using 1/3 point loading,
R	=	f_1/f_2 = a measure of the range of loading stress,
F	=	f_2/f_r = fatigue factor (or stress ratio),
M	=	f_1/f_r = a measure of the minimum stress, and
F_{10}	=	F at ten million repetitions of stress = fatigue strength.

Murdock and Kesler conducted four series of tests with 1/3 point loading. In the first series of tests, the minimum stress was kept constant at 70 psi. The ratio R, therefore, ranged between 0.13 and 0.18. For the other three series of tests, R was kept constant at 0.25, 0.50, and 0.75 respectively.

The influence of range of stress as measured by the ratio R is as follows: for R equal to 0.75, 0.50, 0.25, and 0.13 to 0.18, the fatigue strengths F_{10} are 85, 73, 63, and 61 percent of the static ultimate flexural strength. The results of these tests are shown graphically in Fig 2.3. The S-N curve as determined by Kesler for tests on specimens where the minimum stress was kept constant at zero (R=0) is presented in Fig 2.4.

The accumulation of damage and the rate of crack propagation in concrete is dependent on the rate at which the energy is absorbed. This can be measured by the size of the hysteresis loop due to each cycle of applied load, which is related to the range of the applied stress. This helps to explain why the peak stress that can be sustained increases with an increase in the minimum applied stress.

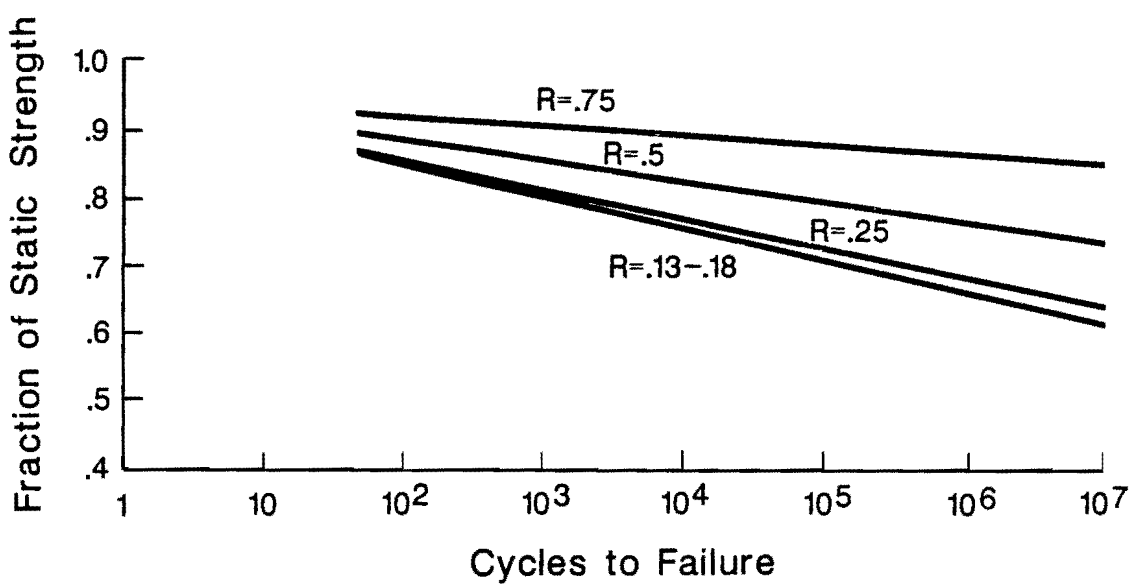

Fig 2.3. Effect of range of loading on fatigue strength of plain concrete beams subjected to repeated loads (Ref 15).

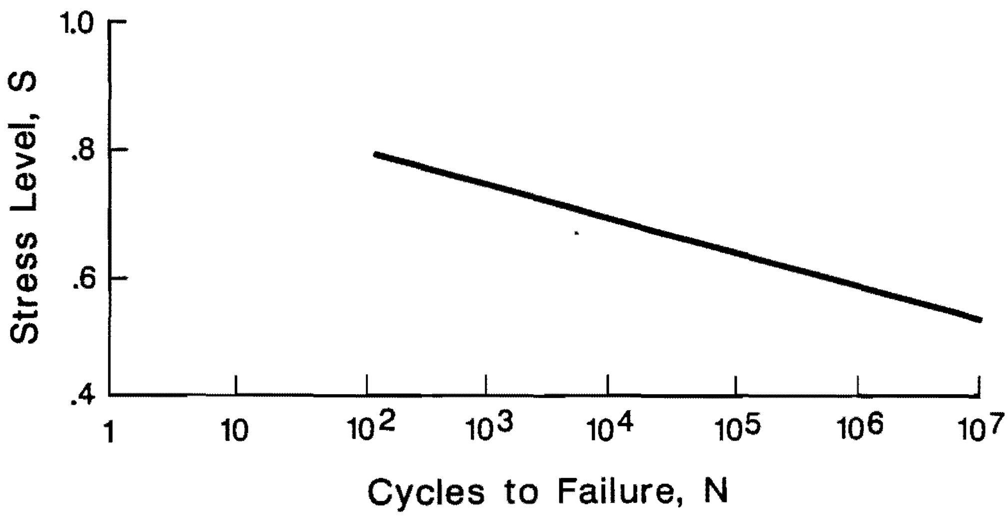

Fig 2.4. Typical fatigue curve for concrete subjected to repeated flexural loading (Ref 6.)

Modified Goodman Diagram

The results of tests by Clemmer and Hatt and Crepps and the effect of range of stress from Murdock and Kesler's studies can be represented by a modified Goodman diagram (Fig 2.5). The ordinates in the diagram represent the fatigue strength at 10 million cycles (F_{10}). The value of M, the ratio of minimum stress to the modulus of rupture, is represented by the 45-degree line passing through the origin. If the value of M is known, then the fatigue strength F_{10} is given by the ordinate of the upper curve with the same abscissa as the corresponding value of M. As the ratio of M is increased, a greater value of fatigue strength can be obtained.

Reversal of Loading

The portion of the modified Goodman diagram that represents the effect of the reversal of loading is only a theoretical approximation based on tests conducted by Hatt and Crepps. It is assumed that if the concrete is subjected to a compressive stress of less than 50 percent of its static compressive strength, the failure of the concrete is caused by the flexural tensile stress. This is because tests by Graf and Brenner indicate that the compressive fatigue strength at 10,000,00 cycles is about 50 percent of its static ultimate compressive strength (Ref 15).

The necessity of verifying the horizontal region of the modified Goodman diagram was obvious to Murdock. He conducted tests on specimens which were subjected to a combination of external axial prestress and flexural loadings. Thus, partial or complete reversal of extreme fiber stresses could be obtained by careful selections of the axial and flexural loadings.

Unfortunately, the results of the tests were inconclusive because of the difficulty in identifying the failure mode. Due to the axially prestressed force, the specimens were able to continue carrying all or a significant part of the applied load despite developing highly visible cracks. When data from early tests showed too much scatter, Murdock discontinued the investigation. Therefore, the horizontal region in the modified Goodman diagram remains unverified as suggested by the dashed line of Fig 2.5.

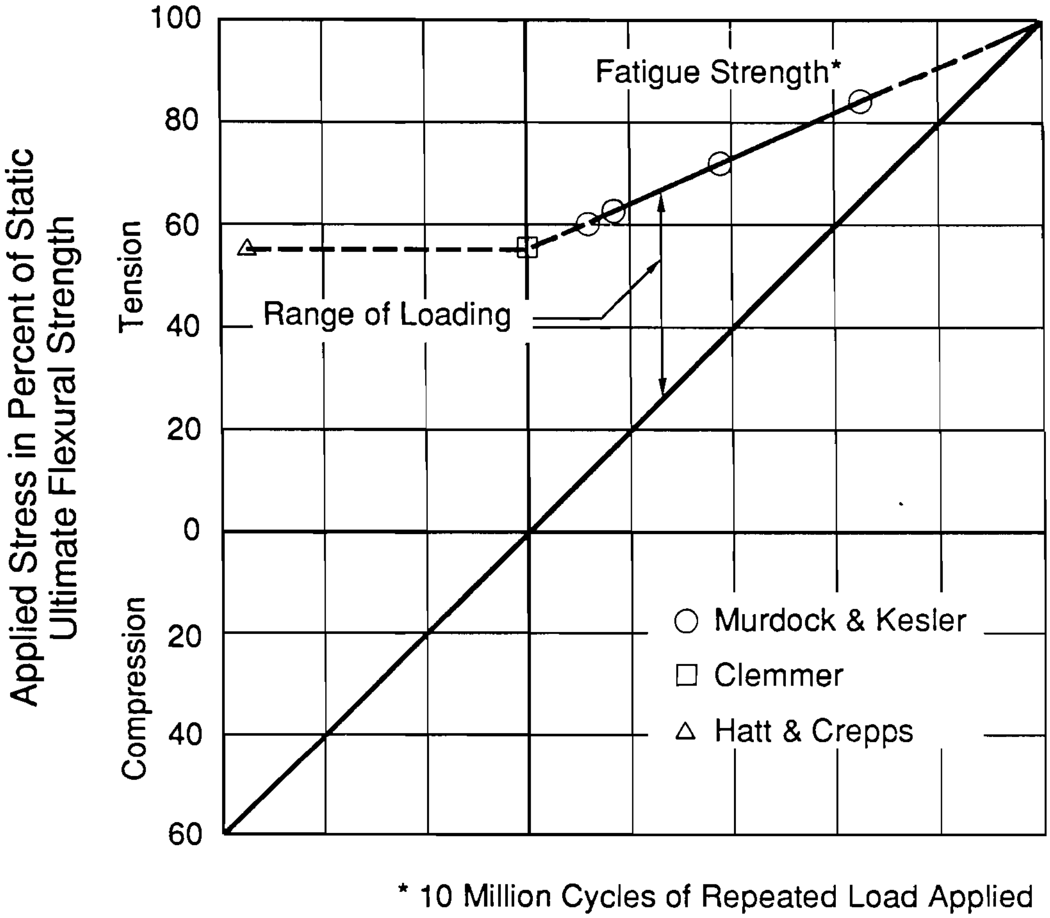

Fig 2.5. Modified Goodman diagram showing the effect of the range of stress on the fatigue strength of plain concrete under 10 million cycles of repeated loading (Refs 6, 16, and 17).

Effect of Rest Periods

The effect of rest periods on the fatigue strength of concrete was first investigated by Hatt (Ref 17). In his tests, the specimens were subjected to overnight and weekend rest periods. When he compared the strain readings before and after the rest periods, he found that an appreciable recovery of deformation had taken place. When testing was stopped for five weeks due to mechanical failure, a specimen which was on the verge of failure completely recovered.

Studies on rest periods were also conducted by Murdock and Kesler and Hilsdorf (Ref 19). Murdock and Kesler's tests on specimens subjected to intermittent 5-minute rest periods and 10-minute loading periods gave strong indication that the rest periods increased the fatigue strength of the concrete, as shown in Fig 2.6.

Hilsdorf conducted a series of tests on specimen which were programmed to have rest periods varying from one to 27 minutes. The specimens were subjected to constant repeated loading where the maximum and minimum stresses were kept constant. During the rest periods, the specimens were subjected to a constant load which was substantially lower than the maximum repeated load. Hilsdorf found that the recovery was rapid in the initial stages of the rest period but the recovery rate quickly diminished. He concluded that no significant benefits could be derived from rest periods in excess of 5 minutes. The results of Hilsdorf's study are shown in Fig 2.7.

Effect of Rate of Loading

The effect of rate of loading on fatigue strength of concrete was investigated by Kesler (Ref 6). He subjected specimens to three different rate of loadings: 70 , 230, and 440 cpm. The results from these tests indicated that the rate of loading has no significant effect on the fatigue strength of concrete.

The results of Kesler's test allow researchers to be more confident in deriving meaningful conclusions from data which can now be accumulated more rapidly.

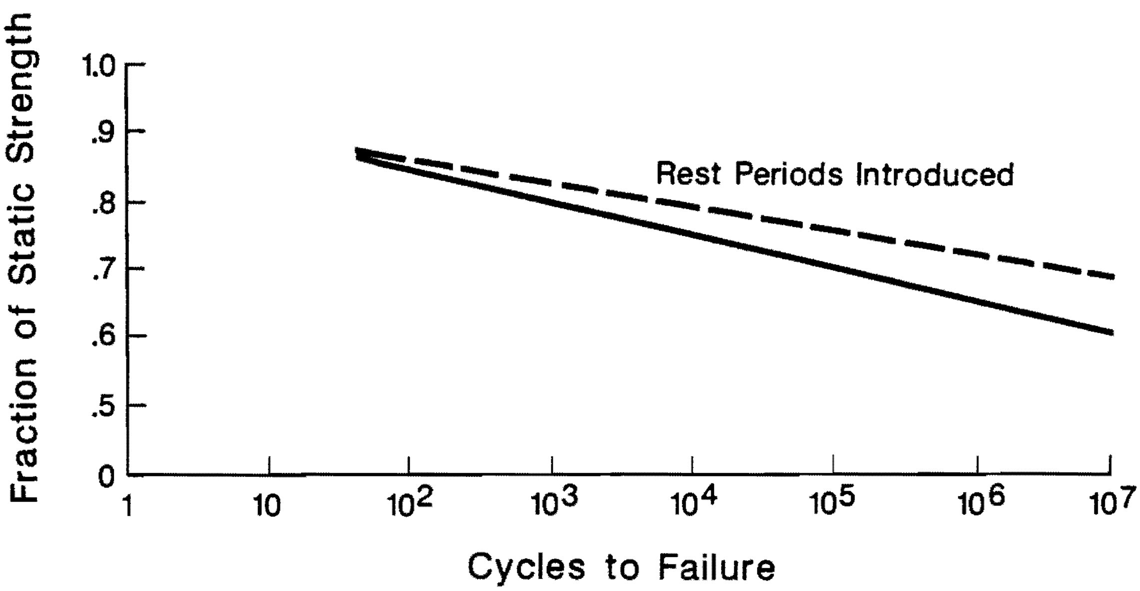

Fig 2.6. Effects of rest periods on the fatigue strength of plain concrete subjected to repeated flexural loads (Ref 15).

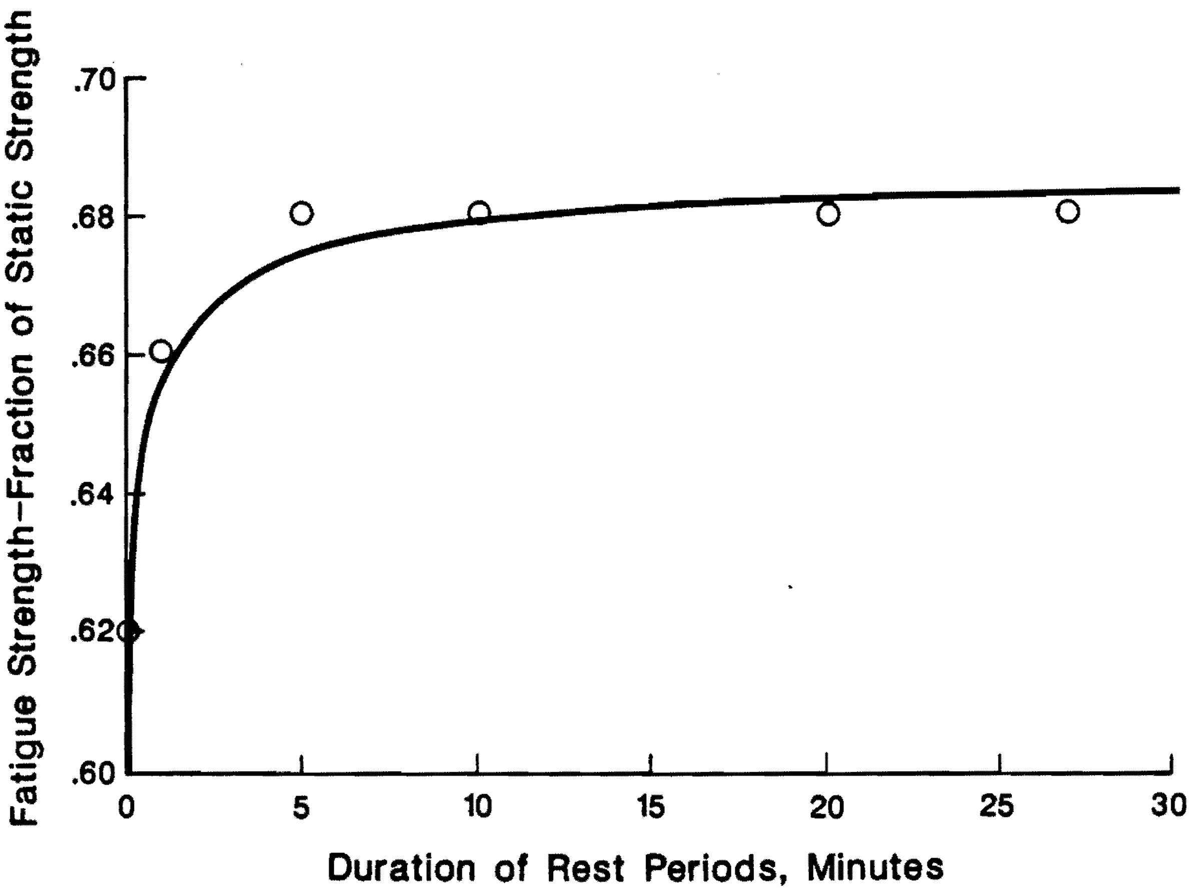

Fig 2.7. Relationship between fatigue strength at ten million cycles and duration of intermittent rest periods (Ref 15).

Probability Concept in Fatigue

In 1958, McCall introduced the concept of probability into the analysis of fatigue data (Ref 20). Until then, all fatigue data were presented in a two-dimensional S-N (stress level vs number of cycles to failure) coordinate system.

McCall carried out tests on twenty air entrained specimens subjected to complete reversal of loading. The specimens were tested at a loading rate of 1800 cpm and the fatigue strength was set at twenty million cycles.

In analyzing his data, McCall first established a relationship between probability of failure and the number of cycles to failure. The relationship between probability of failure and the applied stress level was then determined. The results were then presented in an S-N relationship together with the important third dimension of probability of failure. This is shown in Figure 2.8.

Results of McCall's tests indicated that, with a probability of failure at 0.5, the fatigue strength at twenty million cycles was about 50 percent of static ultimate strength. For probabilities of failure of 0.1 to 0.8, the fatigue strength at twenty million cycles of reversed loadings ranged from 35 to 58 percent of the static ultimate strength.

Critics of McCall's tests indicated that twenty was too small a sample size to give such quantitative results. Also, the small size of the specimens (3 inches x 3 inches x 14.5 inches) used could have resulted in nonuniform stress distribution at the supports and at the points of loading.

However, McCall in introducing the concept of probability into the analysis has added an important third dimension in the presentation of fatigue data.

Miner's Hypothesis

In 1945, Miner proposed a theory for predicting fatigue in metals. Miner's hypothesis states that fatigue damage is accumulated linearly. That is, fatigue failure will not occur if the sum of the ratios of the actual number of applications divided by the allowable number of applications at that corresponding stress level is less than one.

Mathematically, Miner's hypothesis for no fatigue failure can be stated as follows:

$$\sum n_i/N_i < 1$$

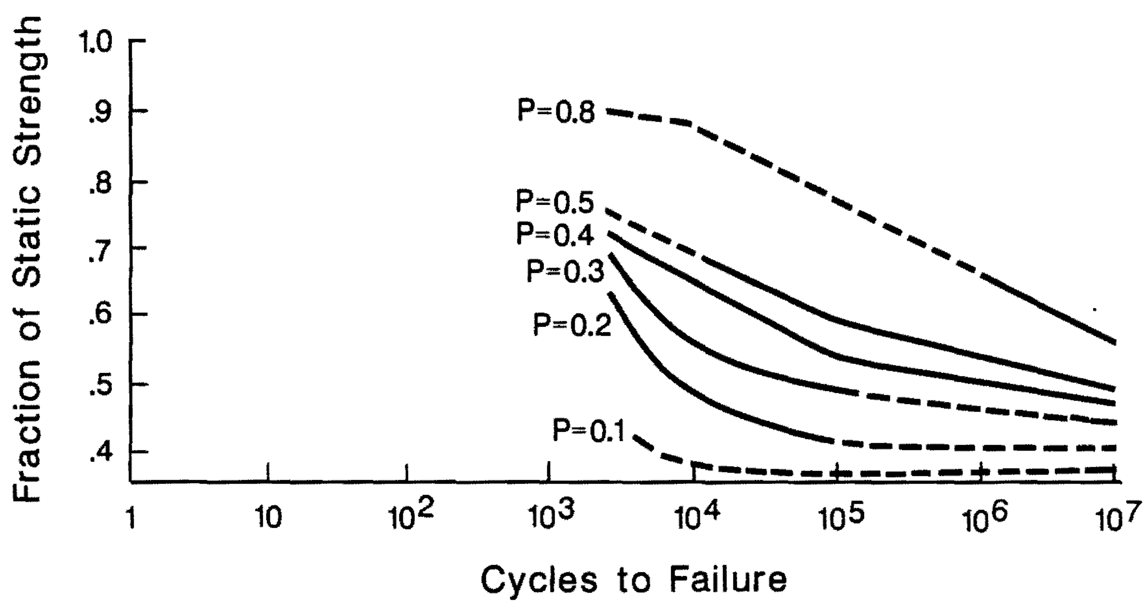

Fig 2.8. S-N curves for various probabilities of failure for plain concrete subjected to reversed flexural loading.

where

n_i = number of load applications at any stress level, and
N_i = allowable number of load applications at the corresponding stress level.

Although the Miner's hypothesis was developed for predicting fatigue failure in metals, most fatigue designs for concrete pavement are also based on Miner's hypothesis. In 1960, Hilsdorf and Kesler carried out an investigation into the validity of applying Miner's hypothesis to fatigue failure in concrete (Ref 19).

Three series of tests were carried out. In the first series of tests specimens were subjected to a specific number of cycles of load at a given stress level. After that, a second stress level, greater than the initial one, was imposed until the specimens failed. In the second series, the order of application was reversed, with the greater stress applied first. In the third series, the two stress levels were continuously alternated until failure. For the third series of tests, the lower stress level was applied first. For the three series of tests, the ratio of minimum stress to maximum stress was kept constant at 0.17. The loading histories are shown in Fig 2.9.

The result of the first test series shows that Miner's hypothesis was not conservative. Specimens subjected to an initial period of high maximum stress level followed by a higher maximum stress level until failure were found to have a shorter fatigue life when compared to fatigue life of specimens which were subjected to continuous loading at the higher maximum stress level.

In the second test series, Miner's hypothesis was found to be conservative. Specimens subjected to an initial period of a high maximum stress level followed by a lower maximum stress level until failure were found to have a greater fatigue life than specimens which were subjected to continuous loading at the lower maximum stress level.

Hilsdorf found that the ultimate tensile strains measured from fatigue test specimens were greater than those observed in static tests. He suggested that the fatigue damage did not accumulate linearly but was dependent on the applied stress level. For a lower stress level, the rate of strain increase was greater at lower ratios of n/N and tended to become more uniform as the ratio of n/N increases. However, for higher stress level, the initial rate of strain increase was small but increased asymptotically as the ratio n/N approached unity.

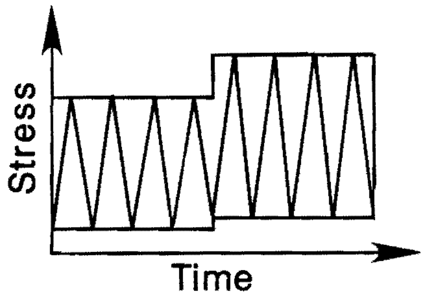

(a) Stress increased once, Program 1.

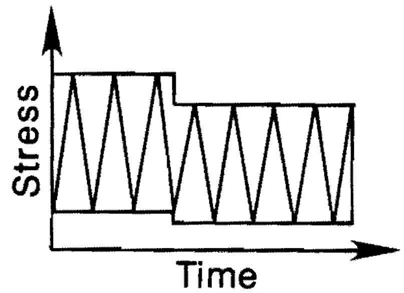

(b) Stress decreased once, Program 2.

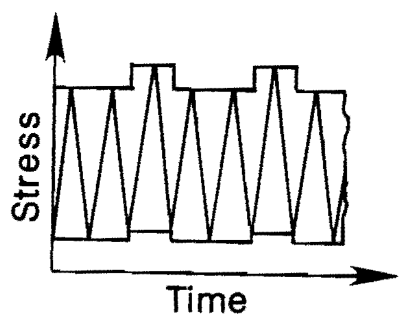

(c) Stress increased and decreased alternately, Program 3.

Fig 2.9. Stress histories investigated by Hilsdorf and Kesler (Ref 21).

These strain measurements provided a logical explanation for the results obtained in the first two series of test. When specimens were subjected to an initial stress level that was low, the accumulated damage was greater than that predicted by Miner's hypothesis. Therefore the fatigue life remaining was reduced. On the other hand, when specimens were subjected to an initial stress level that was high, the accumulated damage was lower than that predicted by Miner's hypothesis. Therefore a greater number of loading cycles at a lower stress level could be applied before failure occurred.

In the third series of tests, Hilsdorf and Kesler found that the fatigue life decreased when the ratio of the number of cycles at the greater stress level to the number of cycles at the lower stress level was increased. Fatigue life also decreased when the difference between the higher and lower stress levels was increased.

In view of the results from the three series of tests, Hilsdorf and Kesler concluded that the assumption of linear accumulation of damage proposed in Miner's hypothesis may not be valid.

Although Hilsdorf presented a fictitious S-N curve (Fig 2.10) with an added third dimension of probability that could more accurately represent Miner's Hypothesis, he cautioned against using it as a design tool.

The studies by Ballinger (Ref 22) also indicated that the Miner's hypothesis reflects the effect of comulative damage due to variability in the fatigue loading in a reasonable manner. For fatigue tests, loads were applied in a sinusoidal pattern at 450 cpm. The ratio of minimum to maximum loads was held constant at 0.15. In the variable load fatigue series, two different levels of loading were applied. The results of this study indicated that the order in which cyclic loads of different magnitudes are applied appears to have no effect on the fatigue life of concrete.

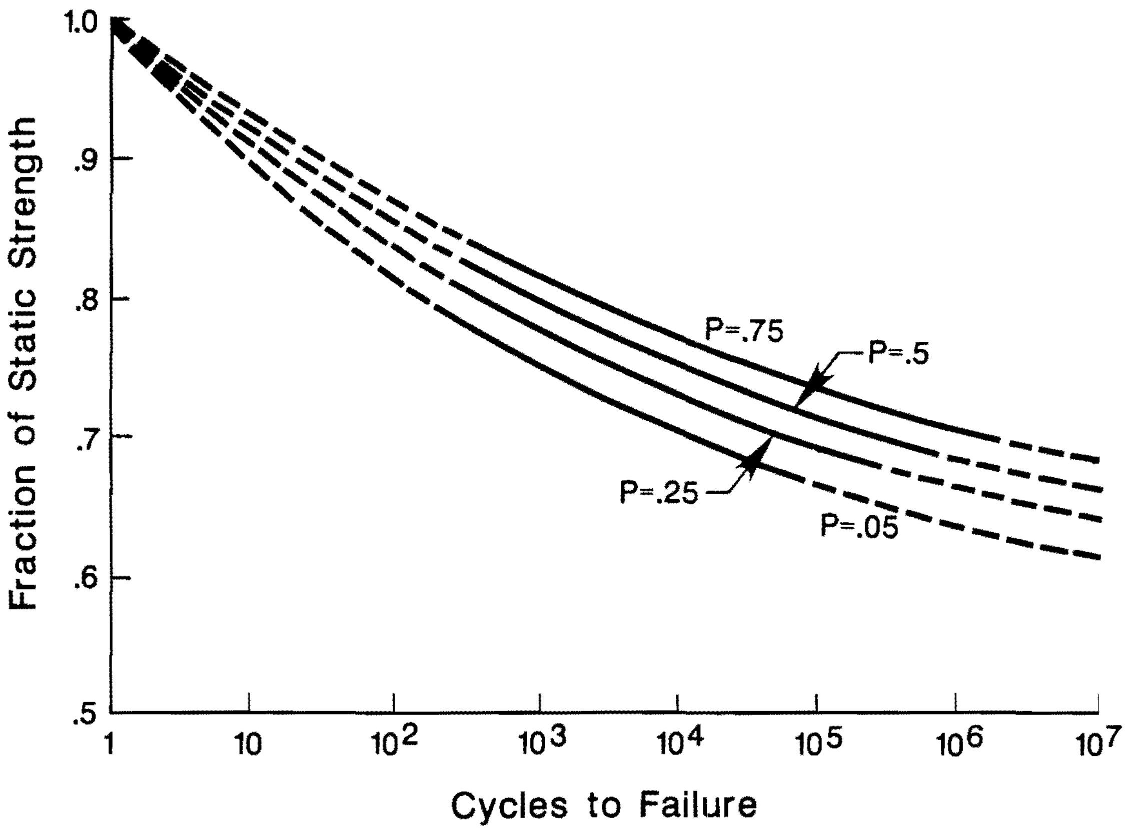

Fig 2.10. S-N curve for various probabilities of failure adjusted for use with Miner's hypothesis.

CHAPTER 3. EXPERIMENTAL PROGRAM TO DETERMINE THE EFFECT OF PRESTRESS ON THE FATIGUE LIFE OF CONCRETE

It was mentioned in Chapter 1 that a re-examination of the data from some prestressed beam tests (28 beams) conducted by the Construction Technology Laboratories, a Division of the Portland Cement Association, shows a strong indication that a small compressive stress may indeed increase the fatigue life of concrete. A similar very limited test program (12 beams) was initiated at The University of Texas at Austin. The main purpose of this preliminary test program was (1) to verify the results from the PCA tests and (2) to identify areas for further research.

DATA FROM PCA TEST

As part of a contract between the Federal Highway Administration and the Portland Cement Association, Construction Technology Laboratories (a division of PCA) was supposed to come up with a five–volume report concerning the design of prestressed concrete pavement.

The data presented here are from volume one, "Prestressed Pavement Joint Designs," of this report. As part of an effort to determine the effect of prestress on concrete fatigue, twenty-eight 6 x 6 x 30-inch concrete beams with a 1/2-inch diameter, 7-wire prestressing tendon centrally located were cast for repeated loading. Plain concrete companion specimens were also cast from each batch for static testing to determine the flexural strength (modulus of rupture) using 1/3 point loading.

Three prestress levels were selected: 50 psi, 100 psi, and 150 psi. The prestress beams were supported on an 18-inch span and were subjected to third point cyclic loading. The applied load was selected to produce a specified fraction (F) of the beam cracking strength. The beam cracking strength was defined as the sum of the flexural strength (f_r) and the prestress (f_p). The values of F selected ranged from 0.7 to 0.9. Therefore, the applied load P can be determined from the formula where

L	=	span length,
b	=	beam width, and
d	=	beam depth.

The load was applied through a hydraulic actuator and the rate of loading was maintained at 300 cpm. To prevent impact, the minimum load for each cycle was set at 100 to 150 lb, instead of zero. Failure was defined as occurring at the first crack. This was detected by the use of a 1/2–inch–wide aluminum strip glued to the extreme tensile fiber (beam bottom surface). The breakage of the aluminum foil due to crack formation will stop the hydraulic system, thereby terminating the test.

The results from these tests were plotted and compared against a fatigue curve derived by Kesler and Murdock and Ballinger. This is shown in Fig 3.1. Based on these comparisons, the authors concluded that "prestress level up to about 25 percent of flexural strength had no evident effect on flexural fatigue life of concrete".

It must be mentioned that the comparison was made with S-N curves determined from tests in which the ratio R (defined earlier in Chapter 2) was kept constant at 0.13 to 0.18. However, with an initial prestress, the specimens in the PCA tests were subjected to a compressive stress before any load is applied. When cyclic loading was then applied to the specimens, the bottom surfaces of the specimens were subjected to a range of loading stresses varying from a minimum stress, which is compressive, to a maximum flexural stress. Therefore, it would be more accurate to compare the data obtained with the S-N curve from Kesler, (Fig 3.4 in Ref 6), where R = 0. This S-N curve is superimposed onto Fig 3.1.

Because the range of loading stresses has a profound effect on the fatigue life of concrete, it can be seen from data points of the PCA tests that the applied prestress resulted in a substantial increase in fatigue life. The data from the PCA tests are statistically analyzed in Chapter 5, to determine whether the increase in fatigue life is proportionately related to the amount of prestress applied.

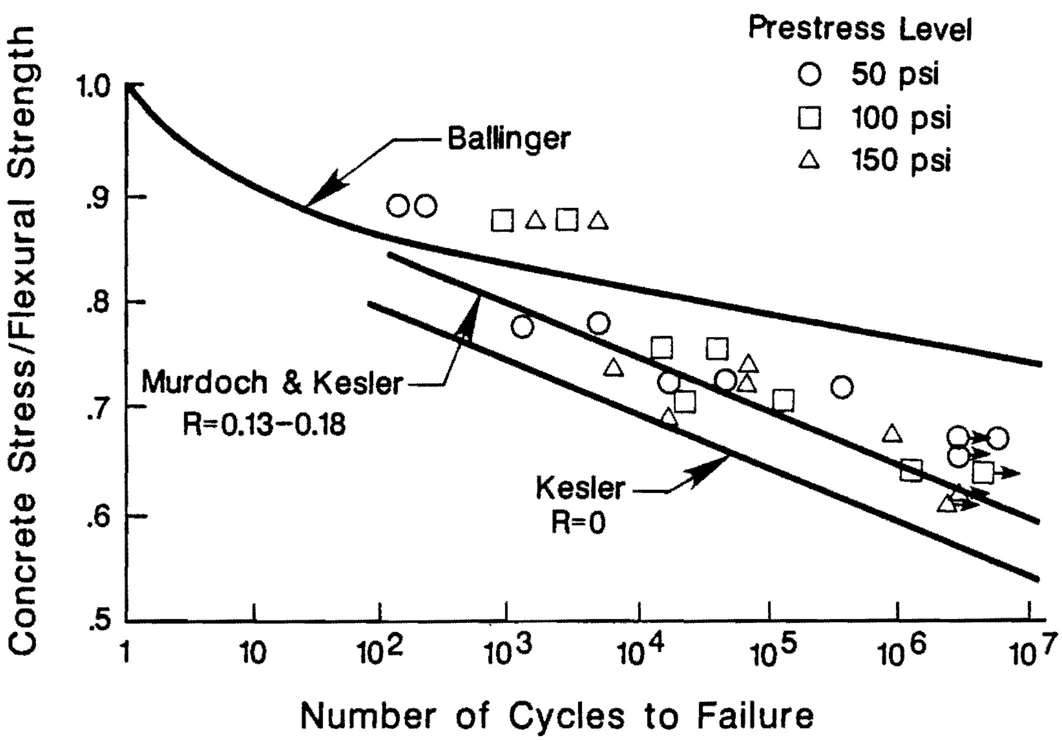

Fig 3.1. Fatigue data from PCA test (Refs 6 and 15).

TEST PROGRAM AT THE UNIVERSITY OF TEXAS AT AUSTIN

In view of the short time available and the scope of this study, a full scale testing program which would have provided statistically sound data was found to be not feasible. Instead, a preliminary test program was initiated to

(1) to verify the results of the PCA investigation,

(2) to increase the data base on the effect of prestress on the fatigue life of concrete, and

(3) to investigate the structural integrity of the prestressed beam after initial cracking.

Experimental Set-up

For this study, twelve 6 x 6 x 42-inch concrete beams with a 1/2-inch diameter, 7-wire strand centrally positioned were constructed for repeated loading. Twenty-four 6 x 6 x 21-inch plain concrete companion specimens and eight cylinders were also cast from the same batch of concrete for static testing to determine the flexural strength and compressive strength respectively.

The original plan was to divide the 12 specimens into three groups of four. Each group was to be tested at the same stress level, with the four specimens having initial prestress applied at 0 psi (unstressed), 50 psi, 100 psi, and 150 psi. Since there were three different groups, three stress levels were selected. The values of f_{rb}/f_r were 0.85, 0.70, and 0.55 as shown in Table 3.1.

After the first group (stress level = 0.85) were tested, the results were found to have too much scatter. In order to obtain more fruitful results from the remaining eight specimens, it was decided to change the amount of prestress applied. Instead of four prestress levels (0, 50, 100, 150 psi), two levels were used. Two beams were stressed to 150 psi and the other two in the same group were stressed to 300 psi. The stress level was also changed, from 0.55 to 0.60. Three main reasons were behind the change in testing procedure:

(1) It was hoped that by testing two specimens with the same prestress level, it would give replicated data, or, at least, provide an average value.

TABLE 3.1. INITIAL TEST PLAN

Stress Level (f_{rb}/f_r)	Prestress Level (psi)			
	0	50	100	150
0.85	1	2	3	4
0.70	5	6	7	8
0.55	9	10	11	12

f_{rb} = resultant stress at bottom fiber
f_r = modulus of rupture

(2) Increasing the difference in the prestress levels applied to the specimens could make the effect of different levels of prestress more noticeable.

(3) The stress level 0.55 was too low and the specimens would probably not fail below 10 million cycles.

Table 3.2 shows the revised testing plan for the remaining eight specimens.

Casting the Specimens

Formwork for casting the specimens consisted of 2 X 8-inch pine wood pieces which were sawed into the desired size. To locate the strand, 11/16–inch holes were drilled into the sides of the forms. To ensure that the prestressing strands were centrally located throughout the specimens, a small prestress force was applied to keep the strands taut. Before the initial stressing operation could be carried out, the white plastic coating and the grease were removed from the strands protruding from the formwork. The strands were then held in place by two prestressing chucks, one at each end. In order to facilitate the easy removal of the chucks, spacer plates were used. The formwork and the stressing operation to keep the strands taut are shown in Fig 3.2. Equipment used in the stressing operation included a hand-operated hydraulic pump, a center-hole ram, a prestressing chair, and two chucks. The section of the strands to be encased by the concrete was enclosed by a white plastic coating to allow the concrete beams to be post-tensioned later.

The type of concrete used was Class S concrete from the Texas State Department of Highways and Public Transportation's 1982 Standard Specifications for Construction of Highways, Streets and Bridges. The concrete was ordered from Texas Readymix and met the following requirements:

(1) minimum beam strength at 7 days - 600 psi (third point test),

(2) minimum 28-day compressive strength - 4000 psi, and

(3) six sacks of cement per cubic yard of concrete.

The coarse aggregate used was 3/4–inch maximum size crushed stone. The concrete had 5 percent entrained air and a 3–inch slump. All the specimens, companion beams, and

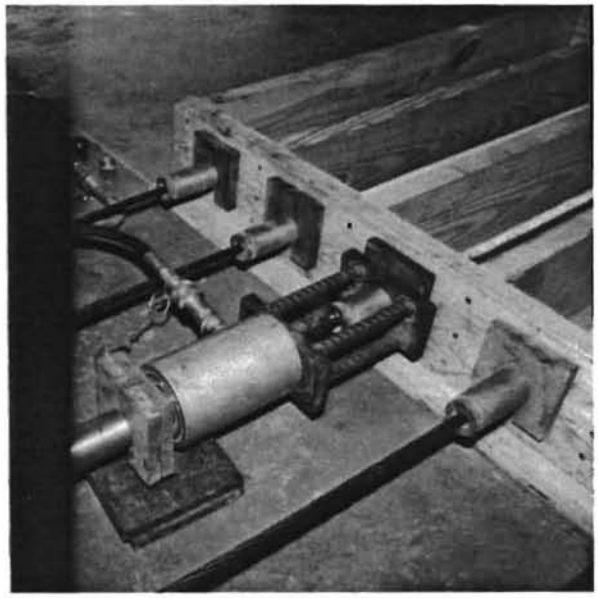

(a) Side view.

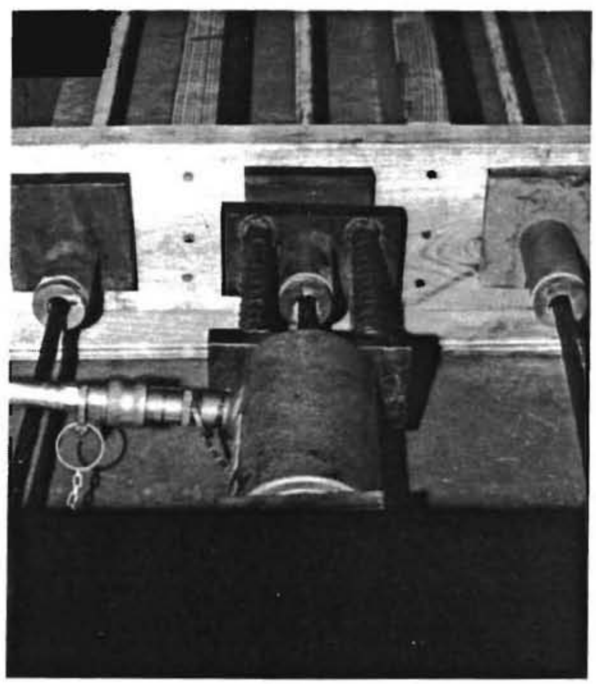

(b) Front view.

Fig 3.2. Initial stressing operation.

TABLE 3.2. REVISED TEST PLAN FOR REMAINING EIGHT SPECIMENS

Stress Level (f_{rb}/f_r)	Prestress Level (psi)			
	0	50	100	150
0.70	6	8	5	7
0.60	10	12	9	11

f_{rb}= resultant stress at bottom fiber
f_r = modulus of rupture

cylinders were cast from the same batch of concrete. The specimens were cast on a Friday, de-molded on the next Monday, and air-cured for 45 days before testing started.

Post-Tensioning the Beams

An important phase in carrying out this study is the post-tensioning of the concrete beams. Because the specimen is so short, take-up losses can be considerable. To ensure that the correct prestress force is applied to the beam, the following equipment is required for the stressing operations

(1) hand operated hydraulic pump with pressure gage,
(2) center-hole ram with 20,000–lb capacity,
(3) prestressing chair with a 5 x 5–inch hole on one side and a 1-inch–diameter hole on the other,
(4) one screw-type prestressing chuck for the stressing end (Fig 3.3),
(5) two normal prestressing chucks, one for anchoring and one for the stressing operation,
(6) two 6 x 6 x 1/4 –inch plates (one for each end) for transferring prestress force to the concrete beam, and
(7) two 4 x 4–inch spacer plates for the stressing and to facilitate removal of the screw–type prestressing chuck after completion of the test and two spacer plates for the stressing operation.

Before the stressing operation, the center hole ram was calibrated . Calibration was carried out by causing the ram to react against a compression cylinder testing machine. The loads corresponding to the gage pressures were then recorded. The step by step procedure for the stressing operation is outlined below:

(1) Ensure that all the white plastic coating that is protruding from the beam is removed. De-grease the strands as much as possible.
(2) Place one of the 6 x 6 x 1/4–inch plates and the normal prestressing chuck on the anchor end of the beam.

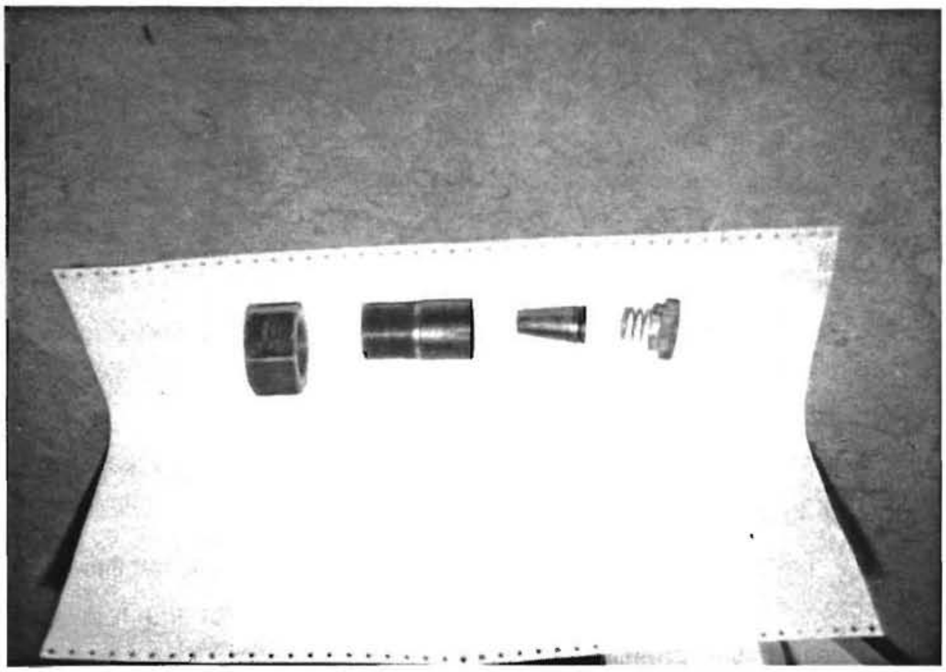

Fig 3.3. Components of screw-type prestressing chucks.

(3) Place the other 6 x 6 x 1/4–inch plate, the two 4 x 4–inch spacer plates, and the screw-type chuck on the stressing end of the beam.

(4) Place the stressing chair with the square hole resting on the end of the beam. Then insert the center-hole ram through the strand with the "piston end" facing outwards. Place two more spacer plates next to the piston end and, finally, place the other prestressing chuck. If the procedure has been correctly carried out, the assemblage will look like that in Figs 3.4 and 3.5.

(5) Carry out the stressing operation. Use the hand operated hydraulic pump; the piston end of the center hole ram will elongate the prestressing strand, because the outer chuck is now gripping the strand.

(6) Read the amount of force that is applied, from the pressure gage, which was calibrated earlier. When the correct gage reading is reached, stop pumping. Due to the elongation of the strand, the screw-type chuck will now not be in contact with the two 4 x 4–inch spacer plate.

(7) Push the screw-type chuck towards the beam, and, using the bolt, screw the chuck tightly against the spacer plate.

(8) Release the pressure from the hydraulic pump. The piston end will return to its original position. The strand wants to return to its original unstressed state but can not because of the screw-type chuck, which effectively transfers a compressive force onto the beam.

(9) Repeat Steps 5, 6, 7, and 8 until the screw-type chuck remains tightly screwed to the spacer plate when Steps 5 and 6 are repeated. When this occurs, the correct amount of prestress force has been transferred to the beam.

(10) After the stressing operation is completed, glue a one–inch–wide aluminum strip to the bottom surface (during testing) of the specimen (Fig 3.4).

<u>Equipment for Fatigue Test</u>

The test set-up is shown in Fig 3.6. The following equipment was used to fatigue test the specimens:

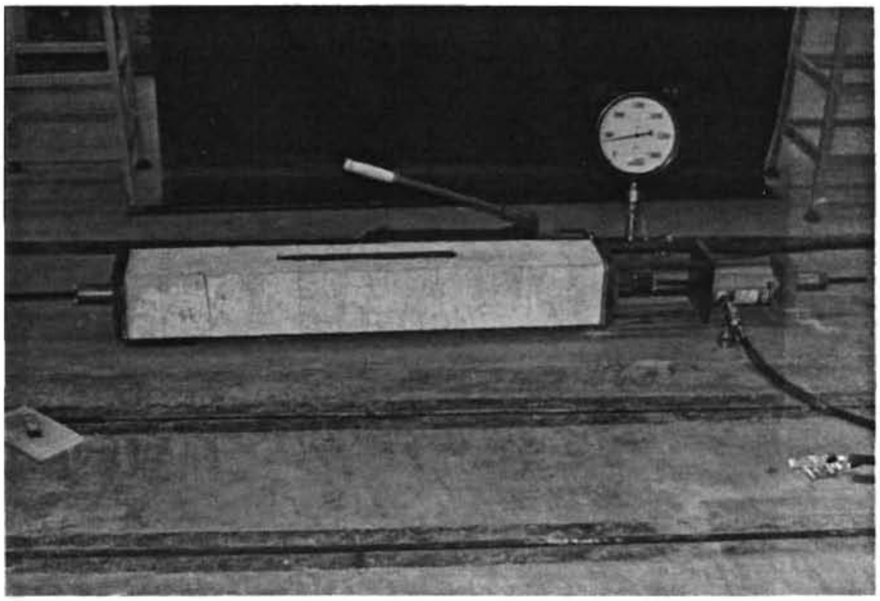

Fig 3.4. Side view of stressing operation.

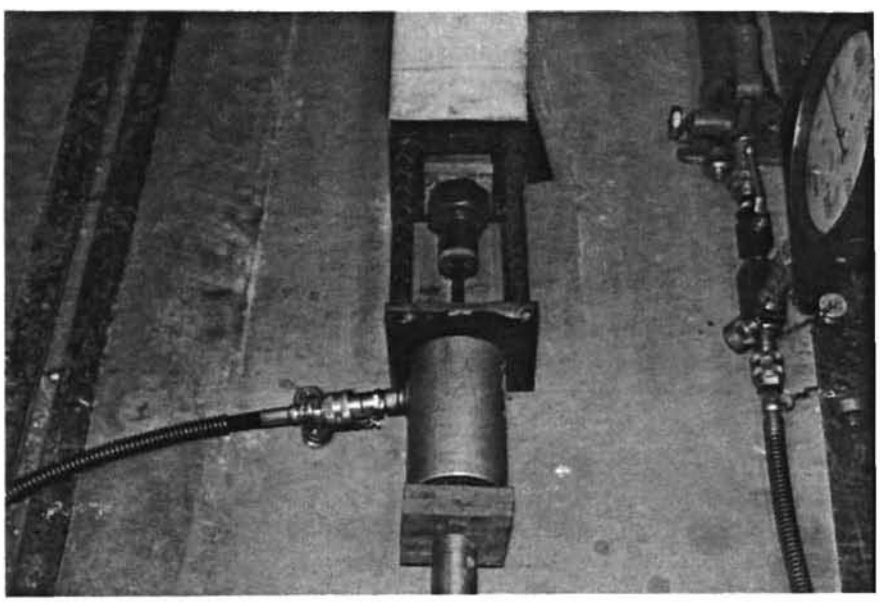

Fig 3.5. Front view of stressing operation.

(1) Two simple supports: each consisted of two L8 x 8 x 1 sections welded together and supported on structural tubing secured to the floor by 12 high-strength bolts. A 1/2–inch–diameter 6–inch–long round bar was welded on top of the two connected channels for the specimen to sit on. Movement to the sides was prevented by four thin steel plates welded to the sides of the round bar.

(2) The loading frame: it consisted of two vertical supports of structural tubing with outer diameter of 4 inches and inner diameter of 3 inches. The horizontal members included two W10 x 15 upper beams and two W12 x 16.5 lower beams connected by a steel truss.

(3) The electronic system: a Material Testing System (MTS), Model 810, including a master control panel (Model 413), a controller (model 442), a digital generator (Model 410), and a counter panel (Model 417) was used to drive the loading actuator (Fig 3.7).

(4) The loading actuator: an MTS Model 34G-E1 fatigue-rated loading actuator, with a 35-kips capacity, was used for loading.

(5) The loading plate: a one–inch–thick plate with two 3/4–inch round bars welded at 12 inches apart was used as the loading plate.

(6) A DCDT resting on a Z-shaped holder for measuring deflection. The Z-shaped holder has a small hole where the top of the DCDT could rest.

(7) Aluminum foil and alligator clips.

Running a Test

Before the first specimen was tested, the load control system and the DCDT were calibrated. The load control system used was a closed-loop hydraulic servo-controlled system as shown in Fig 3.8. By using a National Bureau of Standards (NBS) traceable strain simulator, the electronics of the servo controller were calibrated. Then the 35-kip load cell was placed on a compression testing machine and proof-tested for linearity. It was found that the load cell was linear for the range of loading expected during the fatigue test.

The DCDT was then calibrated, using a micrometer device, as shown in Fig 3.9. One end of the DCDT was connected to the MTS system while the other was attached to the micrometer. Calibration of the DCDT was carried out through the use of the oscilloscope in the MTS system.

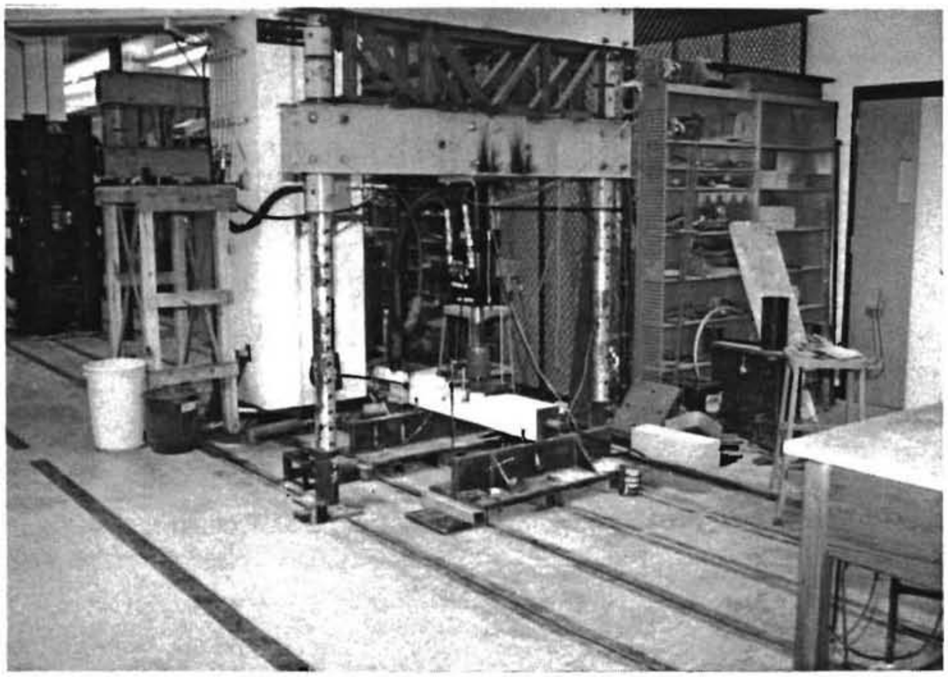

Fig 3.6. Test set-up.

Fig 3.7. MTS electronics system.

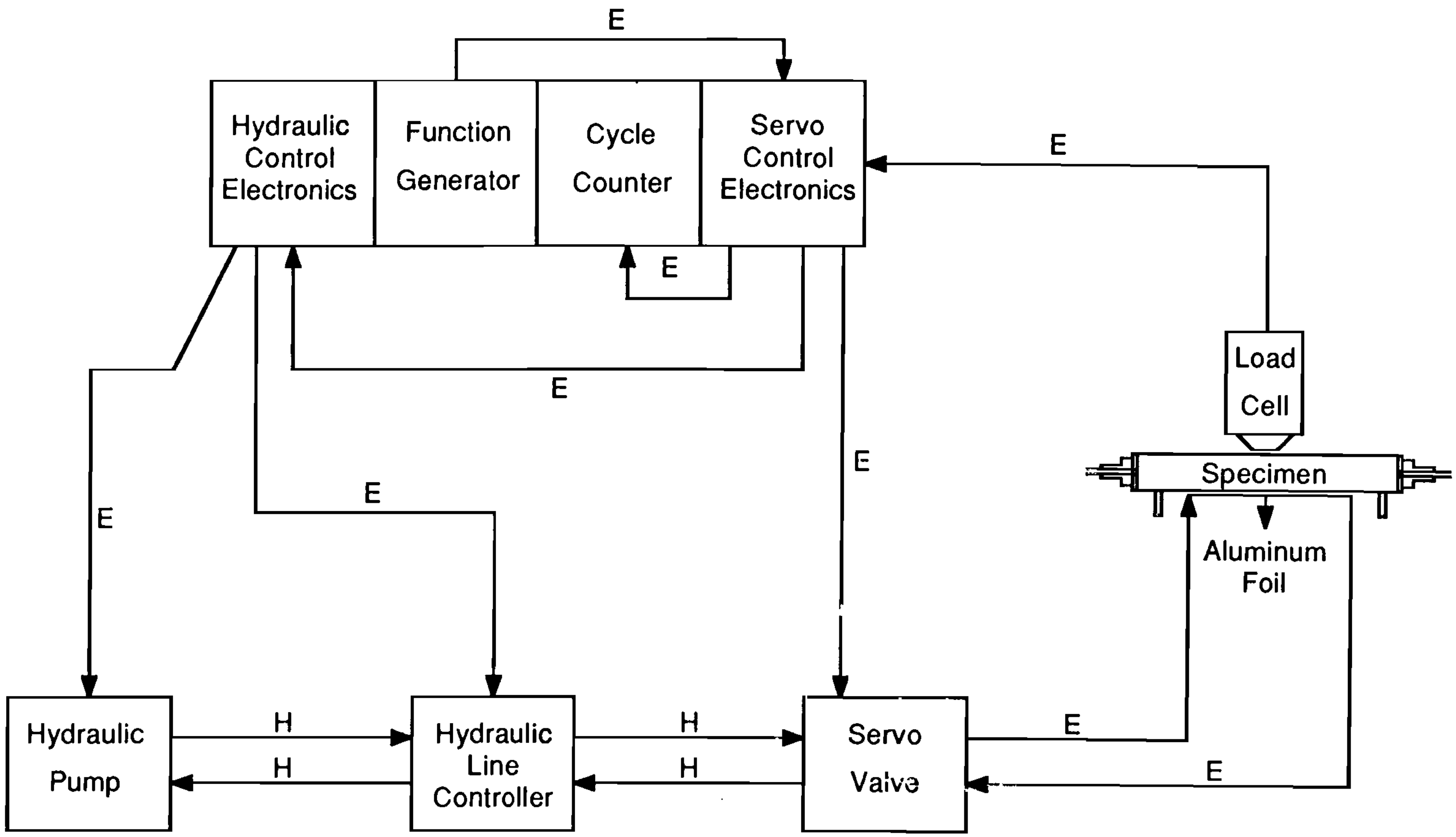

H = Hydraulic Interconnection

E = Electronic / Electrical Interconnection

Fig 3.8. Block diagram: fatigue test servo control system.

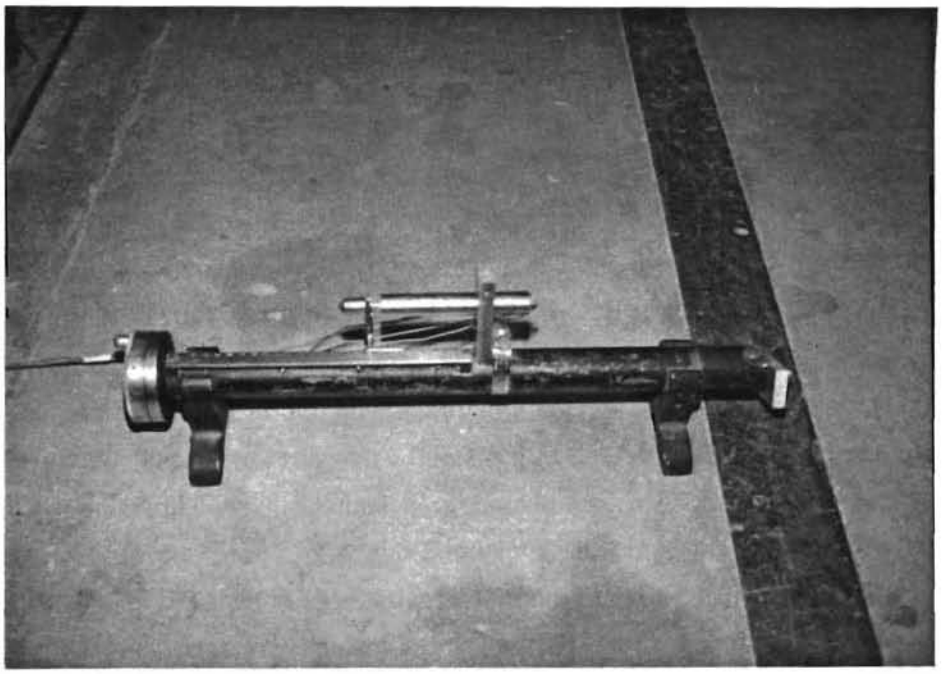

Fig 3.9. Calibrating the DCDT.

The voltage at which the DCDT was calibrated was recorded, and this voltage was maintained for all subsequent tests. The accuracy of the DCDT was 0.001 inch.

The specimen was then placed on the supports, and a Z-shaped holder was epoxied onto the top of the midspan of the specimen (Fig 3.10). The DCDT was placed in position and the voltage was adjusted to the voltage at which the DCDT was calibrated. This voltage was read off from the power supply (right top of Fig 3.7) using a voltmeter.

The loading plate was then placed on the specimen and the loading cell lowered onto the plate. To prevent impact loading, a minimum load of 100 pounds was set. The required minimum and maximum loads (which are explained in Chapter 4) were applied through the master control panel. The electronic loading system is accurate to ±1 pound. The rate of loading was set at 480 cpm.

The midspan deflection was recorded through the oscilloscope. For the shorter tests (high stress level), the midspan deflection was recorded every 500 cycles of loading. For specimens which required several days of testing, deflection readings were recorded every 4 hours from 8 A.M. to 12 midnight. No readings were taken for the period from 12 midnight to 8 A.M.

In order to terminate the test at first crack, the aluminum foil glued to the bottom surface of the specimen was connected to the servo value of the hydraulic unit. This was done by removing the ends of the wire connected to a limit switch which comes with the MTS system. The ends of the wire and the aluminum strips were then connected by alligator clips. This arrangement is shown in Fig 3.11 and is schematically shown in Fig 3.8. When the first crack broke the aluminum foil, the circuit was broken, which stopped the hydraulic system. Since the system was electronically controlled, termination of the test meant that the system recorded the cycle at which the first crack occurred in the specimen.

To continue the test after the first crack, the alligator clips that were attached to the ends of the aluminum foil were now connected. This closed the electrical circuit that was broken due to the breakage of the aluminum foil. Midspan deflection readings were recorded at every 500 cycle until a major crack developed, or when it seemed that the beam was unable to take any more loading.

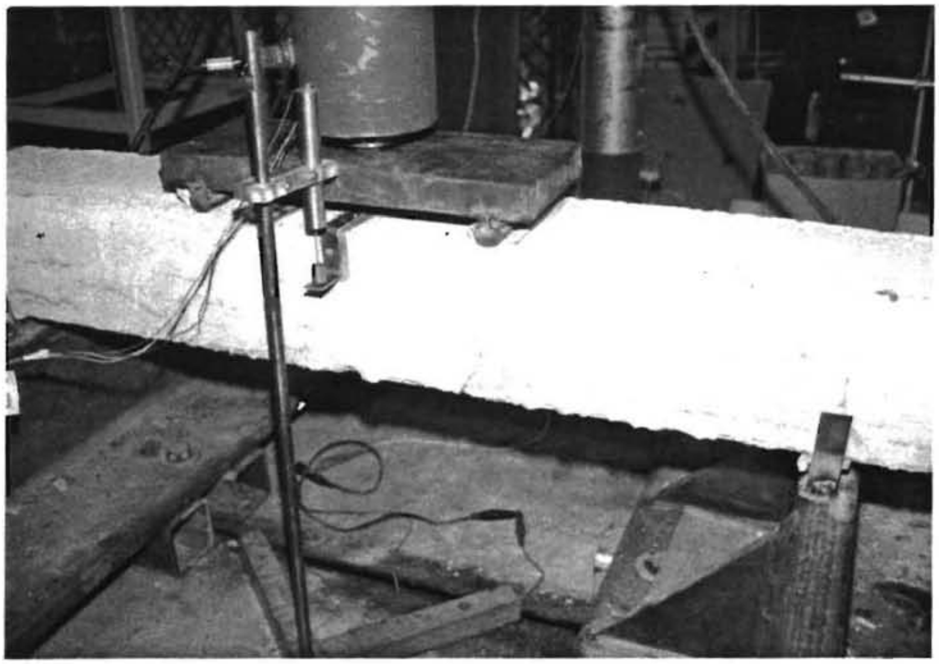

Fig 3.10. Front view of test specimen.

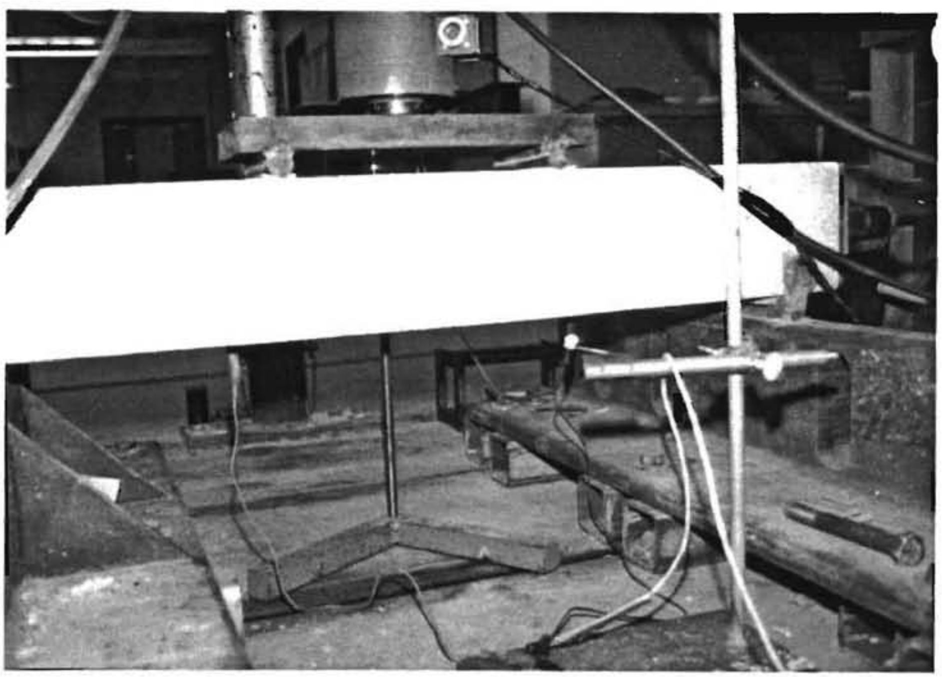

Fig 3.11. Back view of test specimen.

CHAPTER 4. PRESENTATION OF DATA

The results from the experimental test programs at The University of Texas at Austin and from the Portland Concrete Association are presented in this chapter.

MINIMUM AND MAXIMUM LOADS APPLIED

For all the test specimens, the minimum load was maintained constant at 100 pounds. This load was applied to prevent the beam from being subjected to impact loading.

The maximum load to be applied can be determined as follows:

(1) Select the stress level (SL) that the bottom surface of the beam is to be subjected.

(2) Determine the stress at the bottom surface by the equation

$$SL = \frac{f_{rb}}{f_r} = \frac{f_b - f_p}{f_r}$$

or

$$f_b = (SL \times f_r) + f_p \qquad (4.1)$$

where

f_{rb}	=	resultant stress at bottom surface of beam,
f_p	=	applied prestress,
f_b	=	stress at bottom surface of beam due to applied load,
f_r	=	modulus of rupture/flexural strength, and
SL	=	stress level.

(3) Determine the maximum applied load by the equation

$$P_{max} = \frac{bd^2}{L} f_b \tag{4.2}$$

where

P_{max} = maximum applied load,

b = width of specimen,

d = depth of specimen, and

L = span length.

The minimum stress at the bottom surface of the beam due to the 100–pound minimum load is found to be:

$$f_{min} = \frac{P_{min} L}{bd^2}$$

$$f_{min} = \frac{100 \times 36}{6 \times 6^2} = 16.7 \text{ psi} \tag{4.3}$$

Since the applied prestress ranged from 50 to 300 psi, the beam was subjected to loads ranging from a minimum compressive stress varying from 33.3 to 283.3 psi to a maximum resultant tensile stress as defined by $f_b - f_p$. Because the compressive stresses are so small compared to the compressive strength of concrete, it was assumed that the minimum flexural stress the beam was subjected to is zero, and reversal of loading is not considered. Therefore, R, defined as the ratio of flexural stress at minimum load divided by the flexural stress at maximum load, is equal to zero.

DEFINITION OF FAILURE

Unlike fatigue tests on plain concrete specimens where failure is usually synonymous with fracture, some of the prestressed specimens were able to withstand the full applied load despite developing cracks of considerable magnitude. Three kinds of failure were observed during the tests:

(1) First crack, detected by the use of a one-inch strip of aluminum foil. Breakage of the foil interrupted the test.

(2) First development of a major crack, a crack readily visible that appeared to "breathe or pulsate" with each loading cycle. At this point the crack is still below the middepth of the beam.

(3) Propagation of major cracks to failure, evident by the crack propagating across the middepth of the beam and from the noise created by each loading cycle.

The fatigue strengths at the various stress levels were based on failure criterion 1. However, plots of the mid-depth deflection versus number of cycles were from initial loading to ultimate failure, as defined by failure criterion 3. It was found that once the first crack was observed, it took only a few more cycles for a major crack, as defined by failure criterion 2, to develop when testing was resumed.

FATIGUE DATA FROM PCA TEST

In cooperation with the Federal Highway Administration, Construction Technology Laboratories (a division of PCA) conducted fatigue testing on twenty-eight 30 x 6 x 6–inch prestressed beams. The beams were supported on an 18–inch–span and were subjected to third point cyclic loading.

The results from this test are presented in Table 4.1. Three prestress levels were selected: 50 psi, 100 psi, and 150 psi. The applied load was selected to produce a specified fraction (F) of the beam cracking strength, defined as the sum of the flexural strength (f_r)

TABLE 4.1. FATIGUE TEST RESULTS FROM PORTLAND CEMENT ASSOCIATION

Modulus of Rupture (psi)	Prestress Level (psi)	Repeated Load Stress/ Beam Cracking Strength (percent)	Concrete Stress/ Modulus of Rupture (percent)	Number of Cycles to Failure
646	100	70	65	4,320,000*
653	100	80	76	39,800
590	100	70	65	1,140,000
590	100	80	76	13,300
571	100	90	88	2,300
571	100	90	88	870
695	100	75	71	113,000
692	100	75	71	19,800
550	150	70	62	2,200,000*
550	150	70	62	2,190,000*
625	150	80	75	6,340
567	150	75	68	876,000
661	150	80	75	67,900
672	150	90	88	1,650
672	150	90	88	5,050
717	150	75	70	16,800
717	150	75	70	56,200
609	50	70	68	5,190,000
636	50	80	78	4,230
636	50	80	78	1,050
675	50	90	89	170
675	50	90	89	180
590	50	70	67	2,950,000*
590	50	70	67	2,950,000*
610	50	75	73	17,100
610	50	75	73	57,100
668	50	75	73	42,800
668	50	75	73	337,000

*No failure occurred, test was terminated.

and the applied prestress (f_p). The values of F selected range from 0.7 to 0.9. The applied load can be determined as follows:

$$P_{applied} = \frac{(f_r + f_p)\, bd^2}{L} F \qquad (4.4)$$

where

L	=	span length	=	18 inches,
b	=	width of specimen	=	6 inches, and
d	=	depth of specimen	=	6 inches.

It must be mentioned that the selected value of F is not the stress level, which is defined as concrete stress/modulus of rupture. The stress levels have to be calculated. An example is presented below.

Consider the first data point from Table 4.1:

Modulus of Rupture (f_r) = 646 psi
Prestress level (f_p) = 100 psi
F = 0.7

The applied load can be determined by

$$P_{applied} = \frac{(f_r + f_p)\, bd^2}{L} F$$

$$= \frac{(646 + 100) \times 6 \times 6^2}{36} \times 0.7$$

$$= 6274.8 \text{ pounds} \qquad (4.5)$$

The stress at bottom surface of the beam due to the applied load is

$$f_b = \frac{P_{applied} L}{bd^2}$$

$$= \frac{6274.8 \times 36}{6 \times 6^2}$$

$$= 522.9 \text{ psi} \qquad (4.6)$$

The resultant stress at bottom surface is

$$f_{rb} = f_b - f_r$$

$$= 522.9 - 100$$

$$= 422.9 \text{ psi} \qquad (4.7)$$

Therefore the stress level is

$$SL = \frac{f_{rb}}{f_r}$$

$$= \frac{422.9}{646}$$

$$= 0.65 \qquad (4.8)$$

Unlike in the PCA test, the applied load was calculated to produce the required stress level, as explained earlier. The three final stress levels selected were 0.85, 0.70, and 0.60.

The results are presented in Tables 4.2 to 4.4. The fatigue test results based on companion beams cast at the same time as the prestressed beams are presented in Table 4.2. The modulus of rupture results from testing of these companion beams are presented in Table A.1.

When the results from the first series of tests (stress level=0.85) were evaluated based on the modulus of rupture determined from the companion beams, the number of cycles to failure was found to be much higher than expected. One possible explanation was that the flexural strength of the prestressed beams was higher because they were mechanically compacted while the companion beams were hand compacted. It was then decided to conduct static test on the broken "halves" of the failed specimens (Fig 4.1). However, the failure of prestressed specimens at or near the loading points resulted in one of the broken halves having length less than 18 inches long, the minimum length required for a standard flexure test. Therefore some results were based on the modulus of rupture of one of the broken halves of the failed specimens. The results are presented in Table 4.3. Table A.2 presents the results of flexure tests conducted on the broken halves of the failed specimens.

Tables 4.2 and 4.3 are presented in the sequence in which the specimens were tested, while Table 4.4 presents a summary of the fatigue test data.

<u>Mid Span Deflection</u>

Due to a malfunction in the DCDT, readings of the tests conducted at a stress level of 0.85 are not presented. Tables 4.5 through 4.8 present the mid-span deflections for the remaining eigth specimens.

When the beam was in an elastic state, that is before the first crack, the mid-span deflections remained quite constant. Therefore not all the recorded readings are presented. Similarly, for the specimens stressed at 300 psi, the mid-span deflections after the first crack remained quite constant after only a few thousand cycles of loading.

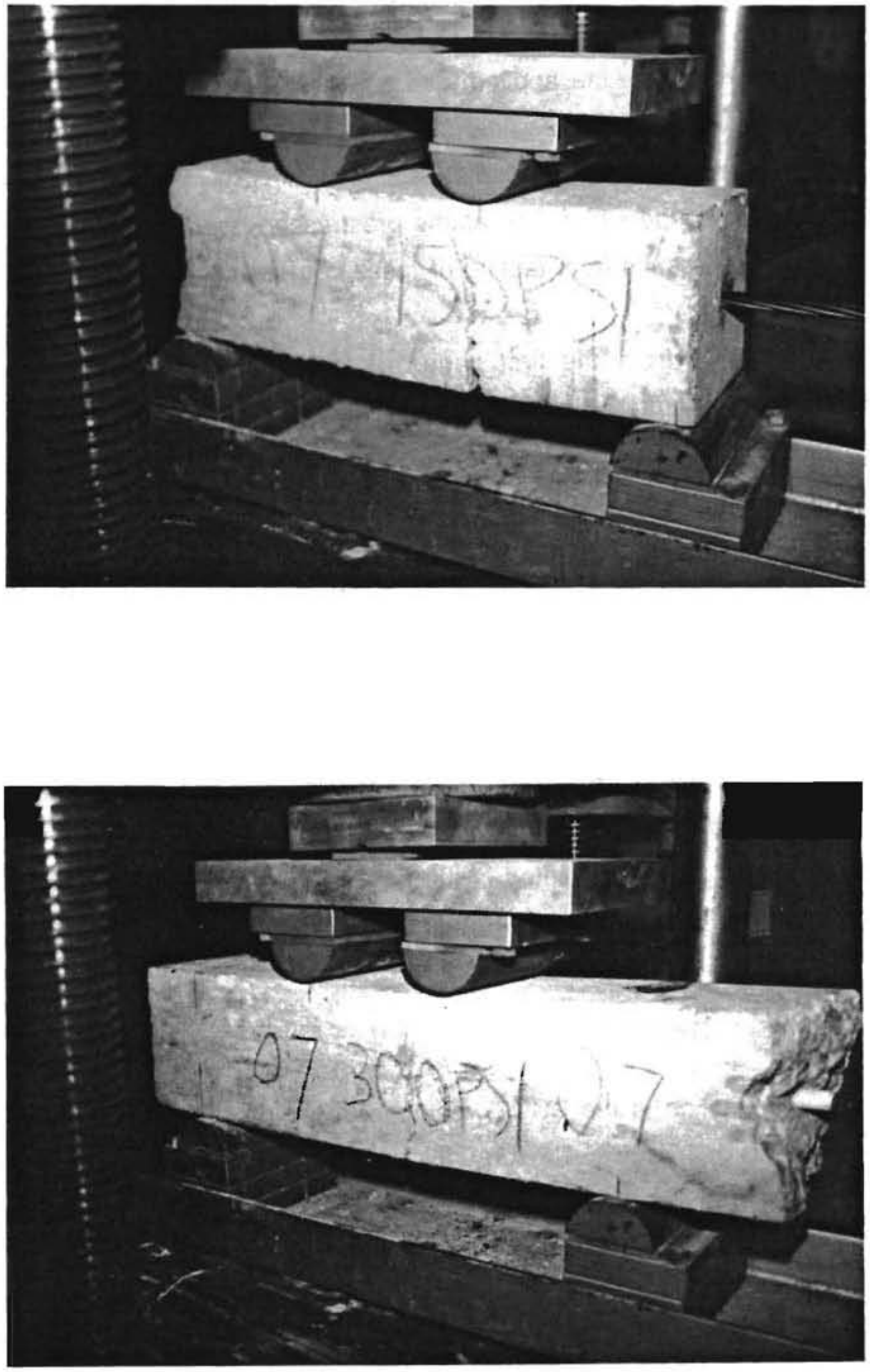

Fig 4.1. Flexure test of broken halves of failed specimen.

TABLE 4.2. FATIGUE TEST RESULTS BASED ON COMPANION BEAMS TESTED AT UT

Specimen Number	Prestress Level (psi)	Modulus of Rupture (psi)	Concrete Stress/ Modulus of Rupture	Number of Cycles to Failure
1	0	583	0.85	13,130
2	50	650	0.85	73,880
3	100	595	0.85	12,400
4	150	613	0.85	131,060
5	300	644	0.70	190,700
6	150	652	0.70	41,570
7	300	688	0.70	91,710
8	150	653	0.70	200,670
9	300	682	0.60	1,393,000
10	150	651	0.60	1,079,400
11	300	654	0.60	1,753,000
12	150	663	0.60	10,000,000*

*No failure occurred, test was terminated.

TABLE 4.3. FATIGUE TEST RESULTS BASED ON BROKEN HALVES OF PRESTRESSED SPECIMEN TESTED AT UT

Specimen Number	Prestress Level (psi)	Modulus of Rupture (psi)	Concrete Stress/ Modulus of Rupture	Number of Cycles to Failure
1	0	677	0.73	13,130
2	50	743+	0.74	73,880
3	100	700+	0.72	12,400
4	150	613+	0.85	131,060
5	300	685+	0.66	190,700
6	150	642	0.71	41,570
7	300	666	0.72	91,710
8	150	672	0.68	200,670
9	300	650+	0.63	1,393,000
10	150	618+	0.63	1,079,400
11	300	638+	0.61	1,753,000
12	150	675	0.59	10,000,000*

*No failure occurred, test was terminated.

+Modulus of rupture based on test of one of the broken halves of failed specimens.

TABLE 4.4. SUMMARY OF FATIGUE TEST RESULTS

	Companion Beam		Broken "Halves"		
Prestress Level (psi)	Modulus of Rupture (psi)	Concrete Stress/ Modulus of Rupture	Modulus of Rupture (psi)	Concrete Stress/ Modulus of Rupture	Number of Cycles to Failure
0	583	0.85	677	0.73	13,130
50	650	0.85	743+	0.74	73,880
100	595	0.85	700+	0.72	12,400
150	613	0.85	613+	0.85	131,060
150	652	0.70	642	0.71	190,700
150	653	0.70	672	0.68	41,570
150	651	0.60	618+	0.63	91,710
150	663	0.60	675	0.59	200,670
300	644	0.70	685+	0.66	1,393,000
300	688	0.70	666	0.72	1,079,400
300	682	0.60	650+	0.63	1,753,000
300	654	0.60	638+	0.61	10,000,000*

*No failure occurred, test was terminated.
+Modulus of rupture based on test of one of the broken halves of failed specimens.

TABLE 4.5. MIDSPAN DEFLECTION READINGS

PRESTRESS LEVEL = 150 PSI STRESS LEVEL = 0.7

Number of Cycles	Deflection (in.) Specimen 6	Number of Cycles	Deflection (in.) Specimen 8
100	0.006	100	0.007
5,000	0.006	5,000	0.007
10,000	0.006	10,000	0.007
15,000	0.006	20,000	0.007
20,000	0.006	30,000	0.007
25,000	0.006	40,000	0.007
30,000	0.006	50,000	0.007
35,000	0.007	60,000	0.007
40,000	0.007	70,000	0.007
41,500*	0.007	80,000	0.007
42,000	0.040	90,000	0.007
42,500	0.045	100,000	0.007
43,000	0.050	110,000	0.007
43,500	0.055	120,000	0.007
		130,000	0.007
	Stopped - crack propagated above middepth of beam - failure criterion 3	140,000	0.008
		150,000	0.008
		160,000	0.008
		170,000	0.008
		180,000	0.008
		190,000	0.008
		200,000	0.008
		200,670*	0.008
		201,000	0.045
		201,500	0.048
		202,000	0.050
		202,500	0.052
		203,000	0.055
		203,500	0.059
			Stopped - crack propagated above middepth of beam - failure criterion 3

*Failure (first crack)

TABLE 4.6. MIDSPAN DEFLECTION READINGS

PRESTRESS LEVEL = 300 PSI STRESS LEVEL = 0.7

Number of Cycles	Deflection (in.) Specimen 6	Number of Cycles	Deflection (in.) Specimen 8
100	0.008	100	0.008
5,000	0.008	5,000	0.008
10,000	0.008	10,000	0.008
20,000	0.008	20,000	0.008
30,000	0.008	30,000	0.008
40,000	0.008	40,000	0.008
50,000	0.008	50,000	0.008
60,000	0.008	60,000	0.008
70,000	0.008	70,000	0.009
80,000	0.008	80,000	0.009
90,000	0.008	90,000	0.009
100,000	0.008	91,710*	0.009
110,000	0.008	92,000	0.037
120,000	0.008	92,500	0.021
130,000	0.008	93,000	0.020
140,000	0.009	93,500	0.018
150,000	0.009	94,000	0.015
160,000	0.009	94,500	0.015
170,000	0.009	95,000	0.015
180,000	0.009	95,500	0.015
190,000	0.009	96,000	0.015
190,700*	0.009	96,500	0.015
191,000	0.025	↓	↓
191,500	0.023		
192,000	0.020		
192,500	0.020		
193,000	0.020		
193,500	0.020	125,000	0.015
194,000	0.020		
194,500	0.020		Stopped - crack remained below middepth of beam - failurecriterion 2
↓	↓		
210,000	0.020		
	Stopped - crack remained below middepth of beam - failure criterion 2		

*Failure (first crack)

TABLE 4.7. MIDSPAN DEFLECTION READINGS

PRESTRESS LEVEL = 150 PSI STRESS LEVEL = 0.6

Number of Cycles	Deflection (in.) Specimen 10	Number of Cycles	Deflection (in.) Specimen 12
100	0.006	100	0.006
1,000	0.006	1,000	0.006
10,000	0.006	10,000	0.006
50,000	0.006	50,000	0.006
100,000	0.006	96,500	0.006
200,000	0.006	100,000	0.007
300,000	0.006	500,000	0.007
400,000	0.006	1,000,000	0.007
500,000	0.006	2,000,000	0.007
600,000	0.006	3,000,000	0.007
700,000	0.006	4,000,000	0.007
800,000	0.007	5,000,000	0.007
900,000	0.007	6,000,000	0.007
1,000,000	0.007	↓	↓
1,079,400*	0.007		
1,080,000	0.032		
1,080,500	0.035		
1,081,000	0.037		
1,081,500	0.040	10,000,000	0.007
1,082,000	0.043		
	Stopped -crack propagated above middepth of beam - failure criterion 3		No first crack occurred

TABLE 4.8. MIDSPAN DEFLECTION READINGS

PRESTRESS LEVEL = 300 PSI   STRESS LEVEL = 0.6

Number of Cycles	Deflection (in.) Specimen 9	Number of Cycles	Deflection (in.) Specimen 11
100	0.008	100	0.007
1,000	0.008	1,000	0.007
10,000	0.008	10,000	0.007
50,000	0.008	50,000	0.007
100,000	0.008	100,000	0.007
200,000	0.008	200,000	0.007
300,000	0.008	300,000	0.007
400,000	0.008	400,000	0.007
500,000	0.009	500,000	0.007
600,000	0.009	600,000	0.007
700,000	0.009	700,000	0.007
800,000	0.009	800,000	0.007
900,000	0.009	900,000	0.008
1,000,000	0.009	1,000,000	0.008
1,100,000	0.009	1,200,000	0.008
1,200,000	0.010	1,400,000	0.008
1,300,000	0.010	1,600,000	0.008
1,393,000*	0.010	1,700,000	0.015
1,393,500	0.010	1,753,000*	0.013
1,394,000	0.010	1,753,500	0.013
1,395,000	0.018	1,754,000	0.013
1,396,000	0.016	1,754,500	0.013
1,397,000	0.013	1,755,000	0.013
1,398,000	0.012	1,756,000	0.013
1,399,000	0.012	1,757,000	0.013
1,400,000	0.012	1,758,000	0.013
	0.012	1,760,000	0.014
	0.012	1,800,000	0.014
		1,900,000	0.014
↓	↓	2,000,000	0.014
		2,100,000	0.014
		2,200,000	0.014
		2,300,000	0.014
1,500,000	0.012	2,400,000	0.014
		2,500,000	0.014
	Stopped -crack remained below middepth of beam - failure criterion 2		Stopped - crack remained below middepth of beam - failure criterion 2

CHAPTER 5. DISCUSSION AND ANALYSIS OF DATA

In this chapter, regression analyses are carried out for the data presented in Chapter 4. Among the topics discussed in this chapter are (1) effect of the prestress level on the fatigue life of concrete, (2) dynamic and static stresses, (3) comparison of plain and prestressed concrete strength, and (4) midspan deflections and failure modes.

REGRESSION ANALYSIS OF PCA'S DATA

The data from the PCA tests are presented in Fig 5.1. In order to determine the effect of prestress on the fatigue life of the concrete, the regression analyses were carried out to determine a best-fit line for the various prestress levels. In the PCA tests, the run-out point for stopping the test was not set at any specific number of cycles. For example, testing was terminated for two specimens at 2,200,000 cycles, for two specimens at 2,950,000 cycles, and for one specimen at 4,320,000 cycles. Yet, one specimen was tested for 5,190,000 cycles, until it failed.

In order to make sense of the data, three seperate least-square regression analyses were run on the data points. The procedures and reasons for each analysis are given here.

Regression Analysis 1 (RA1)

Procedure: All the data points were used. Specimens that did not fail were assumed to have 5,000,000 cycles of loading at failure.

Reason: 5,000,000 cycles was selected because all the specimens for which testing was terminated were subjected to stress levels of less than 0.68. A specimen tested at a stress level of 0.68 failed at 5,190,000 cycles.

Regression Analysis 2 (RA2)

Procedure: All the data points except those for the specimens that did not fail were analysed.

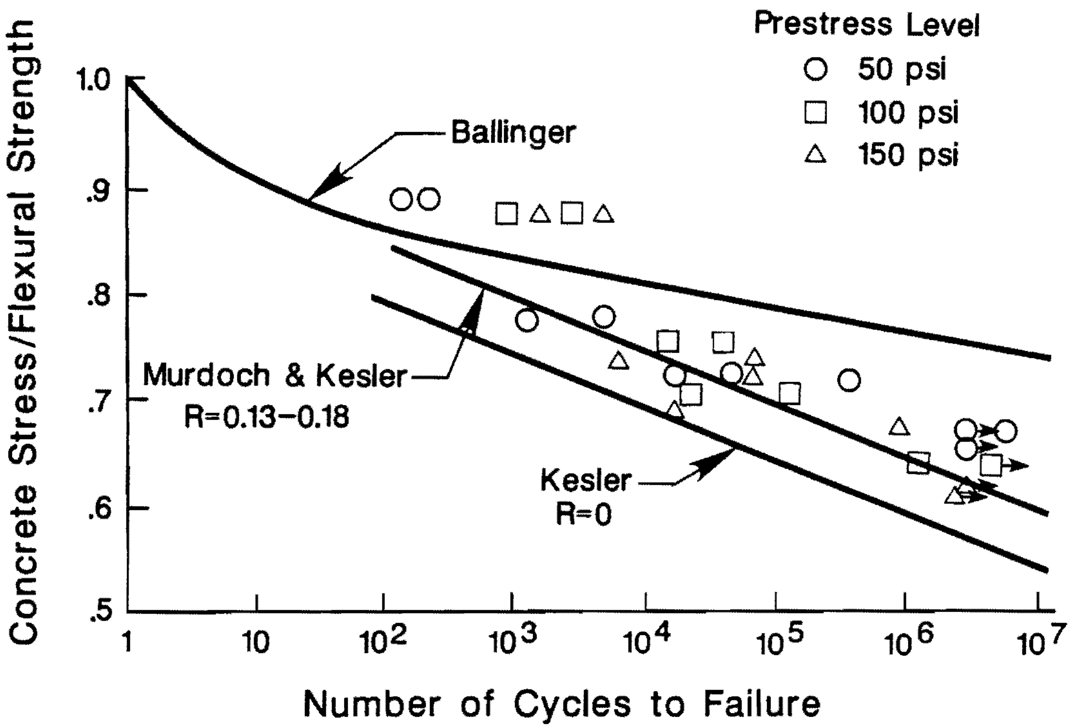

Fig 5.1. Fatigue data from PCA test (Ref 9).

Reason: Since the actual number of cycles at failure was unknown, unfailed samples were left out of the analysis.

Regression Analysis 3 (RA3)

Procedure: All the data points used in RA1 except those for specimens that were tested at a stress level greater than 0.85 were used in the analysis.

Reason: It has been found in fatigue testing of plain concrete specimens that, as the stress level gets higher (greater than 0.85), the relationship between the stress level and the log number of cycles becomes non-linear. Using these data points would make the slope much steeper.

The equations derived from the regression analyses are presented in Appendix B. To show the effect of the different levels of prestress on the fatigue life of concrete, the equations were superimposed on one graph. The results from the three separate analyses are presented in Figs 5.2 to 5.4.

Remarks on Regression Analysis 1 (RA1)

In deriving the three equations for the three different prestress levels, it was found that a good coefficient of correlation existed between the stress level and the logarithm of the number of cycles to failure. For prestress levels of 50, 100, and 150 psi, the coefficient of correlations were -0.93, -0.92, and -0.88 respectively.

From Fig 5.2 it can be seen that the equations derived for prestress levels of 100 and 150 psi are nearly the same and that both equations have a much steeper slope than the equation for the 50 psi prestress level. The two equations for 100 and 150 psi intercept the equation for 50 psi at about the 40,000 to 50,000–cycle range, and at a stress level of about 0.75.

Remarks on Regression Analysis 2 (RA2)

The coefficients of correlation were high for the equations derived for the 50 and 100 psi prestress level. For the 50 psi specimens, the coefficient of correlation was -0.91,

Prestress Level, psi	Regression Equation	Coefficient of Correlation
50	SL=0.9480–0.0427 LogN	–0.93
100	SL= 1.0530–0.0654 LogN	–0.92
150	SL=1.0481–0.0650 LogN	–0.88

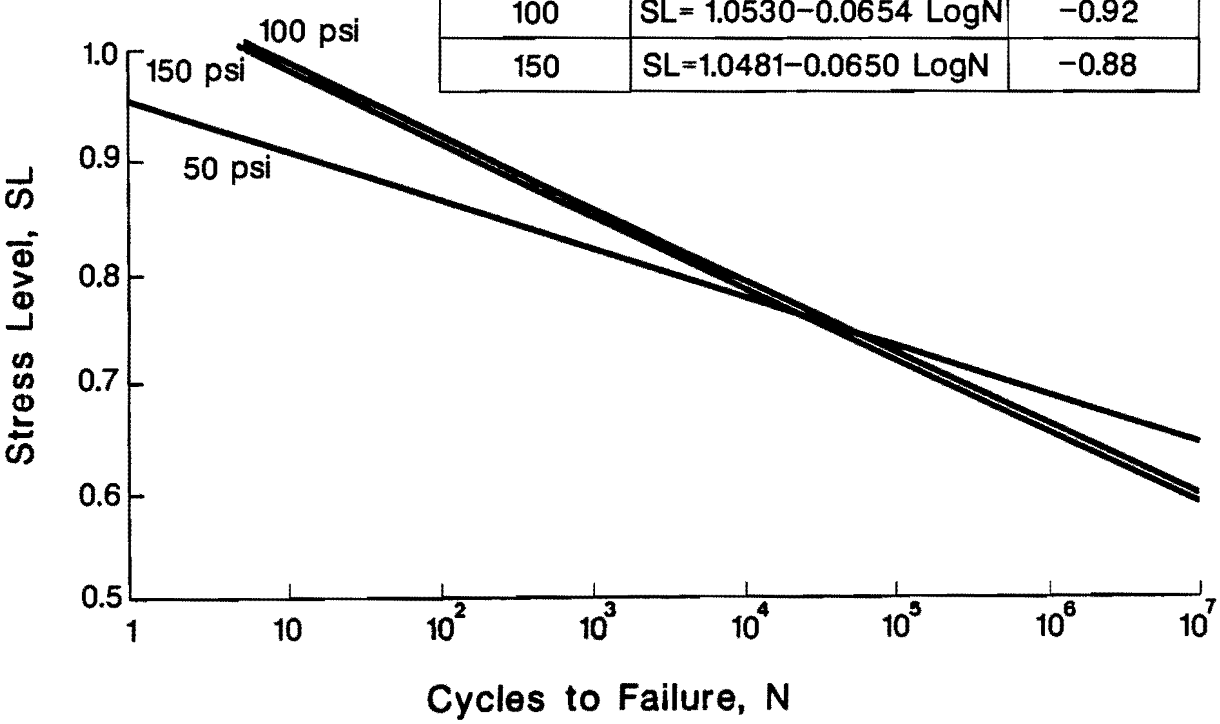

Fig 5.2. Effect of different levels of prestress on fatigue life of concrete based on Regression Analysis 1 (RA1).

Prestress Level, psi	Regression Equation	Coefficient of Correlation
50	SL=0.9565-0.0451 LogN	-0.91
100	SL=1.1030-0.0781 LogN	-0.93
150	SL=1.0770-0.0722 LogN	-0.78

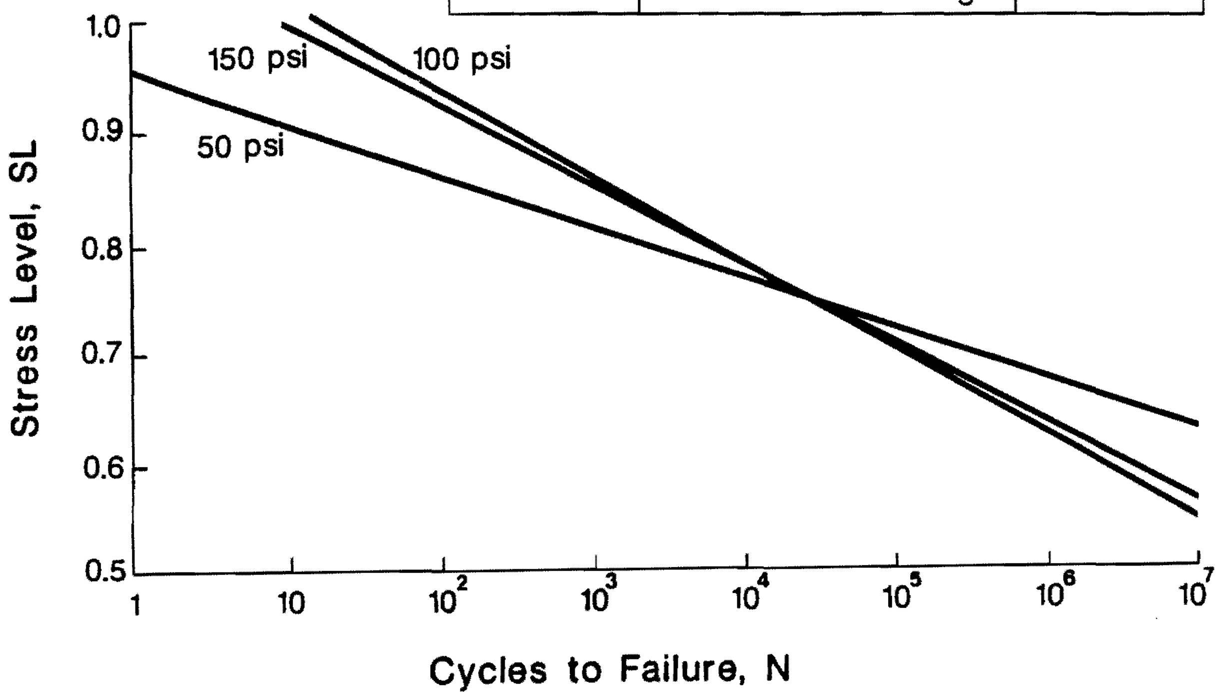

Fig 5.3. Effect of different levels of prestress on fatigue life of concrete based on Regression Analysis 2 (RA2).

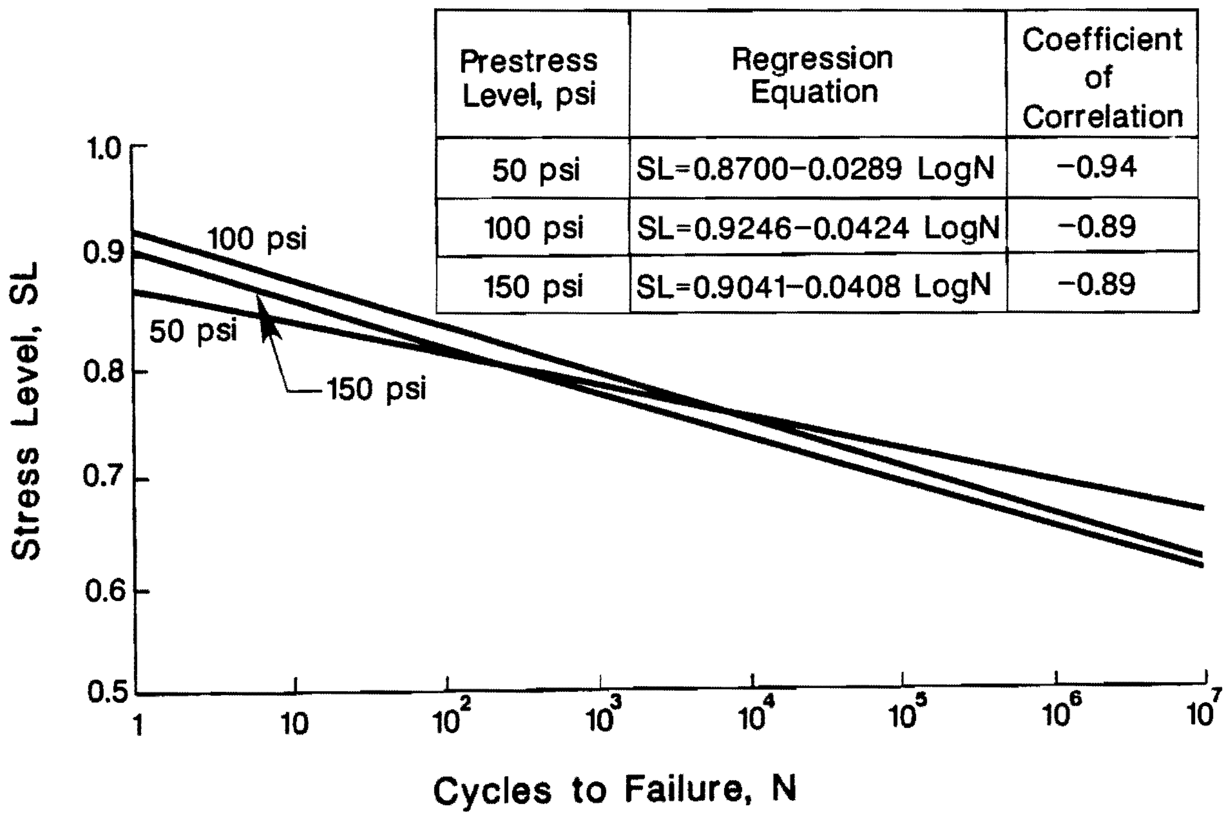

Prestress Level, psi	Regression Equation	Coefficient of Correlation
50 psi	SL=0.8700−0.0289 LogN	−0.94
100 psi	SL=0.9246−0.0424 LogN	−0.89
150 psi	SL=0.9041−0.0408 LogN	−0.89

Fig 5.4. Effect of different levels of prestress on the fatigue life of concrete based on Regression Analysis 3 (RA3).

and for the 100 psi equation it was -0.93. However, the coefficient of correlation for the 150 psi equation was only -0.78.

From Fig 5.3, it can be seen that the 100 psi equation has a slightly steeper slope than the 150 psi equation. Both equations have a much steeper slope than the 50 psi equation. Similar to those for RA1, the 100 and 150 psi equations intercept the 50 psi equation at about the 40,000 to 50,000–cycle range and at a stress level of about 0.75.

Remarks on Regresion Analysis 3 (RA3)

When data points for specimens tested at a stress level greater than 0.85 were excluded from the analysis, the three equations derived had much smaller negative slopes. Similar to those for RA1 and RA2, the 100 psi equation has the highest slope (-0.0424), although it is only slightly steeper than the 150 psi equation (-0.0408). Again, both equations have much steeper slopes when compared to the 50 psi equation (-0.0289).

The coefficients of correlation for the 50 psi, 100 psi, and 150 psi equations were good, and were -0.94, -0.89, and -0.89, respectively. The 50 psi and 100 psi equations intercept at about the 10,000–cycle point and at a stress level of about 0.75, while the 50 psi and 150 psi equations intercept at about the 900–cycle point and at a stress level of about 0.8. The 100 psi and 150 psi equations do not intercept each other.

REGRESSION ANALYSES ON UNIVERSITY OF TEXAS TEST RESULTS

The results of the tests conducted at The University of Texas at Austin are presented in Figs 5.5 and 5.6. Fatigue test results based on modulus of rupture of companion beams are shown in Fig 5.5. Fatigue test results based on modulus of rupture of broken halves are shown in Fig 5.6.

It can be seen that the results based on broken halves have considerably less scatter and seem to verify the test results from the PCA test. However, unlike the PCA data which clustered around the line derived by Murdock and Kesler (R=0.13-0.18), most of the results from this test program lie within the boundaries of the R=0.13-0.18 line and the R=0 line.

In view of the lesser scatter in the results based on the broken halves , a least square analysis was carried out for the data points of the 150 psi and 300 psi specimens. However,

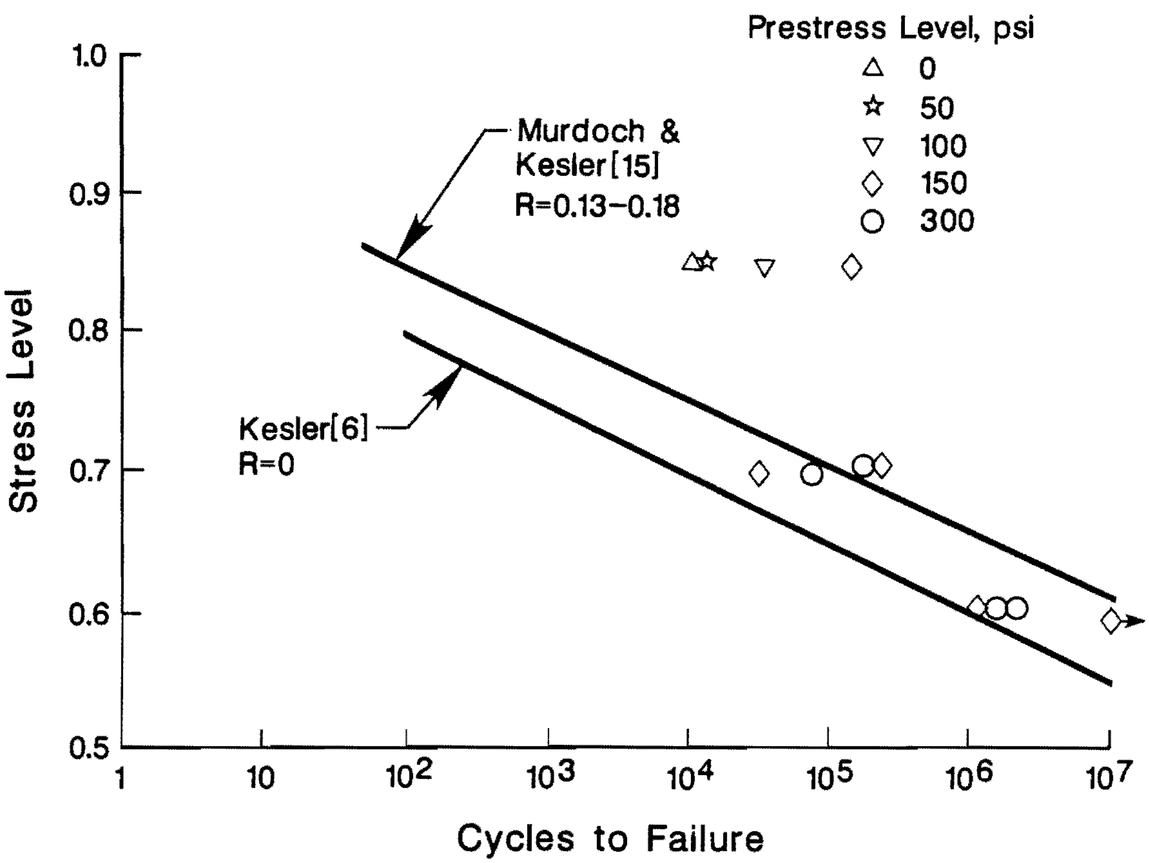

Fig 5.5 Fatigue test results based on companion beams.

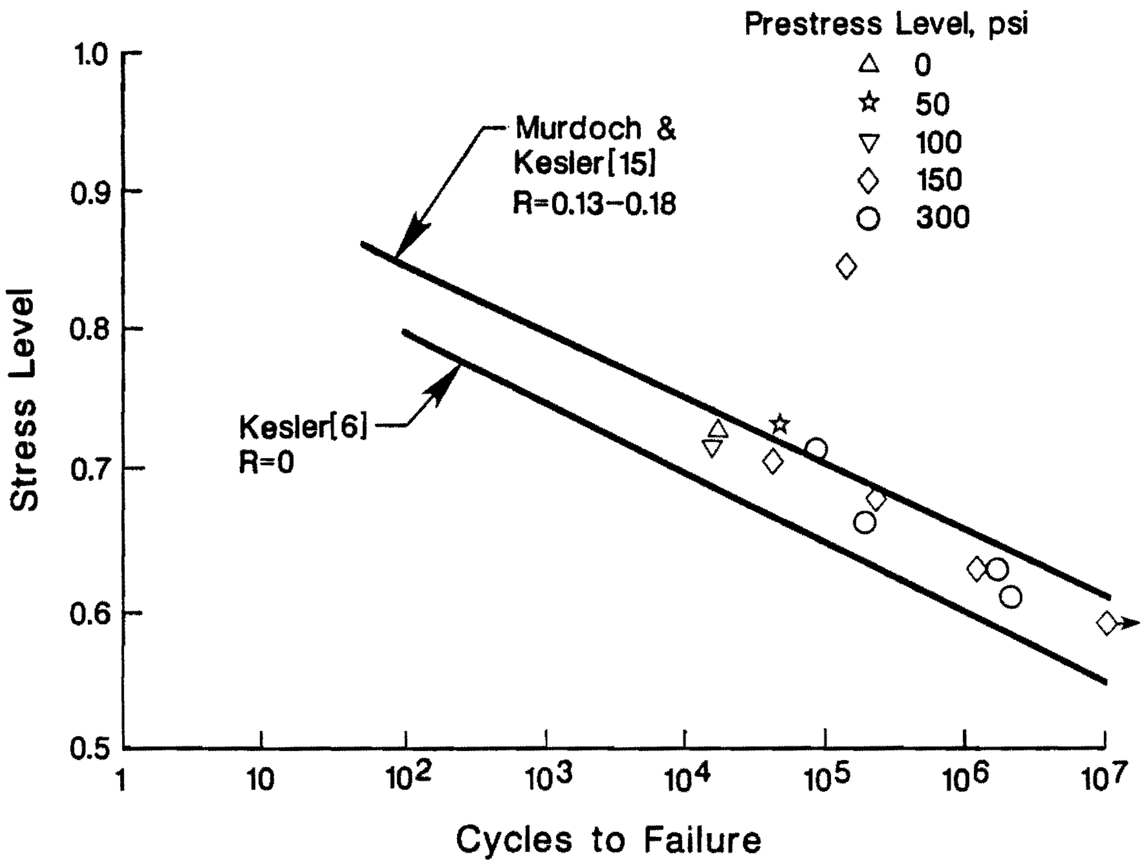

Fig 5.6. Fatigue test results based on broken halves of prestressed specimen.

it must be mentioned that only four sets of data points for each prestress level were available for the analysis. This is quite a small sample size.

The two equations derived are presented in Fig 5.7. It can be seen from Fig 5.7 that the 300 psi equation has a much steeper slope than the 150 psi equation. The two equations intercept at about the 600,000-cycle point and at a stress level of about 0.65.

For the small number of data points, the coefficients of correlation were high. For the 150 psi and 300 psi equations, the coefficients of correlation were -0.99 and -0.94, respectively.

EFFECT OF PRESTRESS LEVEL ON FATIGUE LIFE OF CONCRETE

Based on the results of the regression analysis, the following general comments can be made about the effect of prestress level on the fatigue life of concrete:

(1) The application of a small prestress (50 psi to 300 psi) will increase the fatigue life of concrete.

(2) The slope of the equation representing the relationship between stress levels and the logarithm of number of cycles at failure will increase (be steeper) with an increase in the amount of prestress applied.

(3) In comparing the fatigue life of concrete specimens stressed at the various prestress levels, it was found that the stress level to which the beams were subjected has a profound effect on the fatigue life:

    (a) Comparison between 50 psi and 100 psi specimens: When the specimens were subjected to a stress level greater than 0.75, the 100 psi specimens were found to have a higher fatigue life. For specimens subjected to a stress level less than 0.75, the 50 psi specimens were found to have a higher fatigue life.

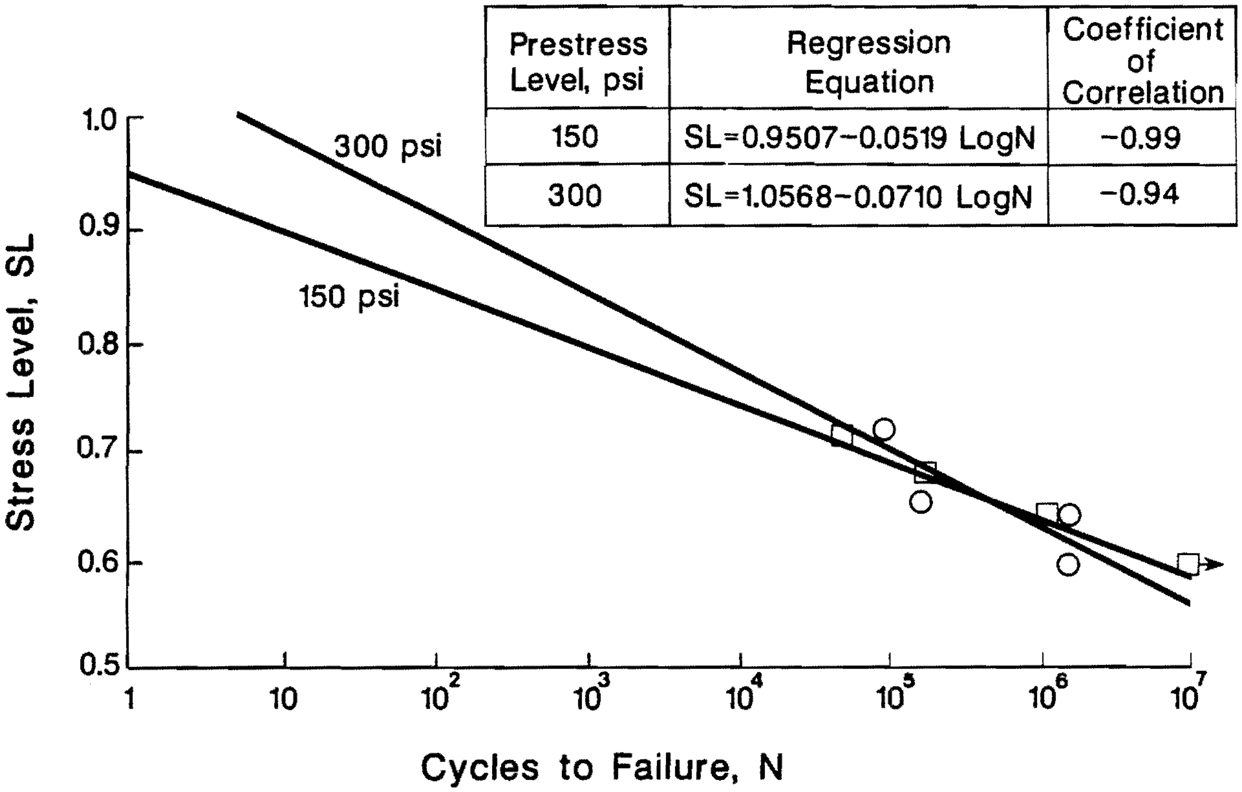

Prestress Level, psi	Regression Equation	Coefficient of Correlation
150	SL=0.9507−0.0519 LogN	−0.99
300	SL=1.0568−0.0710 LogN	−0.94

Fig 5.7. Regression analysis on fatigue test results from The University of Texas at Austin.

(b) Comparison between 50 psi and 150 psi specimens: When the specimens were subjected to a stress level greater than 0.8, the 150 psi specimens were found to have a higher fatigue life. For specimens subjected to a stress level less than 0.80, the 50 psi specimens were found to have a higher fatigue life.

(c) Comparison between 150 psi and 300 psi specimens: When the specimens were subjected to a stress level greater than 0.65, the 300 psi specimens were found to have a higher fatigue life. For specimens subjected to a stress level less than 0.65, the 150 psi specimens were found to have a higher fatigue life.

FATIGUE LIMIT FOR PRESTRESSED CONCRETE

The results from the regression analysis showed that no fatigue limits exist for the concrete beams subjected to 50 to 300 psi of external prestress.

FATIGUE STRENGTH OF PLAIN AND PRESTRESSED CONCRETE

For comparing the fatigue strengths of plain concrete and prestressed concrete, the stress level at a fatigue strength of 10 million cycles was used as a criterion.

The fatigue strength at 10 million cycles (F_{10}) was found in the regression analysis of the PCA data and is presented in Tables B.1 through B.3. The fatigue strengths from the PCA data and The University of Texas results are summarized below:

(1) PCA

Prestress Level	RA1	RA2	RA3	Average Stress Level
0 psi	- -	- -	- -	*0.550
50 psi	0.649	0.641	0.668	0.652
100 psi	0.595	0.556	0.628	0.593
150 psi	0.593	0.572	0.619	0.595

(2) The University of Texas at Austin

Prestress Level	Stress Level
0 psi	0.550
150 psi	0.587
300 psi	0.560

The results show that all the prestressed specimens have a higher fatigue strength than plain concrete. However, as the prestress level increases, the fatigue strength decreases. This is unexpected, as a higher prestress level was conjectured to have a more profound effect in delaying the propagation of the microcracks. A possible explanation can be found in the relationship between the dynamic effect of the applied loading and the static effect of the external prestress. This is explained in the next section.

DYNAMIC AND STATIC STRESSES

In the testing of plain concrete, it was found that the range of applied stress has a profound effect on the fatigue life of concrete. The applied stress was dynamic in nature for all cases.

Unlike with plain concrete, the testing of prestressed concrete beams resulted in the interaction of static and dynamic stresses. While the applied prestress is static in nature, the

---

*University of Texas at Austin Data PCA had no test at 0 psi.

applied loading stress is dynamic. To illustrate the difference, compare the loading stresses required to produce a stress level of 0.75 for the 50 psi and 100 psi beams. Assume the modulus of rupture is 700 psi. To find the loading stress required, use the formula derived in Chapter 4:

$$f_b = (SL \times f_r) + f_p$$

where

f_p = applied prestress,
f_r = modulus of rupture,
f_b = stress at bottom of surface due to applied load, and
SL = stress level.

For 50 psi beams:

$$f_b = (0.75 \times 700) + 50 = 575 \text{ psi}$$

For 100 psi beams:

$$f_b = (0.75 \times 700) + 100 = 625 \text{ psi}$$

Even though the stress level is 0.75 for both cases, the 100 psi specimens were subjected to a higher variation in dynamic stress in every loading cycle. If the stress level is maintained constant, a beam with a higher prestress level will therefore be subjected to a higher range of dynamic stresses, compared to a beam at a lower prestress level.

The propagation of cracks depends on the energy absorption rate, which is related to the size of the hysteresis loop on each cycle of the applied stress. This helps to explain why the lines representing the 50 psi and 100 psi equations cross each other. The conjecture that a higher prestress will have a more profound effect on delaying crack propagation is therefore not violated. This can be seen in the upper left sections of Figs 5.2 through 5.4 and in Fig 5.7.

The propagation of microcracks therefore is dependent on two factors:

(1) the benefits of prestressing and

(2) the accumulated detrimental effects of higher variation in dynamic stresses.

When the beams are subjected to a high stress level, which means the beams will fail at a low number of loading cycles, the benefits of the prestress will have a more profound effect than the accumulated detrimental effects caused by the larger variation in dynamic stresses. When the beams are subjected to a low stress level, which means the beams will fail after a large number of loading cycles, the accumulated detrimental effects in the larger variation of dynamic stresses will override the benefits of the prestress.

The relationship between the benefits of prestressing in delaying crack propagation and the detrimental effects of higher dynamic stress variation is best explained pictorially, as shown in Fig 5.8. Since the prestress force is a statically applied loading, the benefit derived from prestressing should be constant throughout the life of the concrete beam. This is shown in Fig 5.8 as a straight horizontal line. According to Miner's hypothesis, fatigue damage accumulates linearly. As the specimens are subjected to more loading cycles, the accumulated damage increases linearly, as shown in Fig 5.8.

While it can be seen that an increase in prestress increases the benefits by delaying crack propagation, the exact relationship between prestress level and benefit cannot be conclusively determined from the regression analysis. Similarly, the accumulated detrimental effects due to higher dynamic stress variation cannot be conclusively ascertained. Figure 5.8 presents a comparison of the benefits and accumulated detriments of the beam prestressed at 50 and 100 psi.

The horizontal benefit line represents the net benefit of the higher prestress to the 100 psi beam over the 50 psi beam. The linearly increasing line represents the accumulated detrimental effect due to the higher dynamic stress variation on the 100 psi specimen over the 50 psi specimen. The two lines intercept at approximately 50,000 cycles of loading. This corresponds to a stress level of 0.75 (Figs 5.2 and 5.3). Therefore, any specimens prestressed at 100 psi and subjected to a stress level greater than 0.75 will have a higher fatigue life than specimens prestressed at 50 psi and tested at the same stress level. Similarly, any specimens prestressed at 100 psi and subjected to a stress level less than 0.75

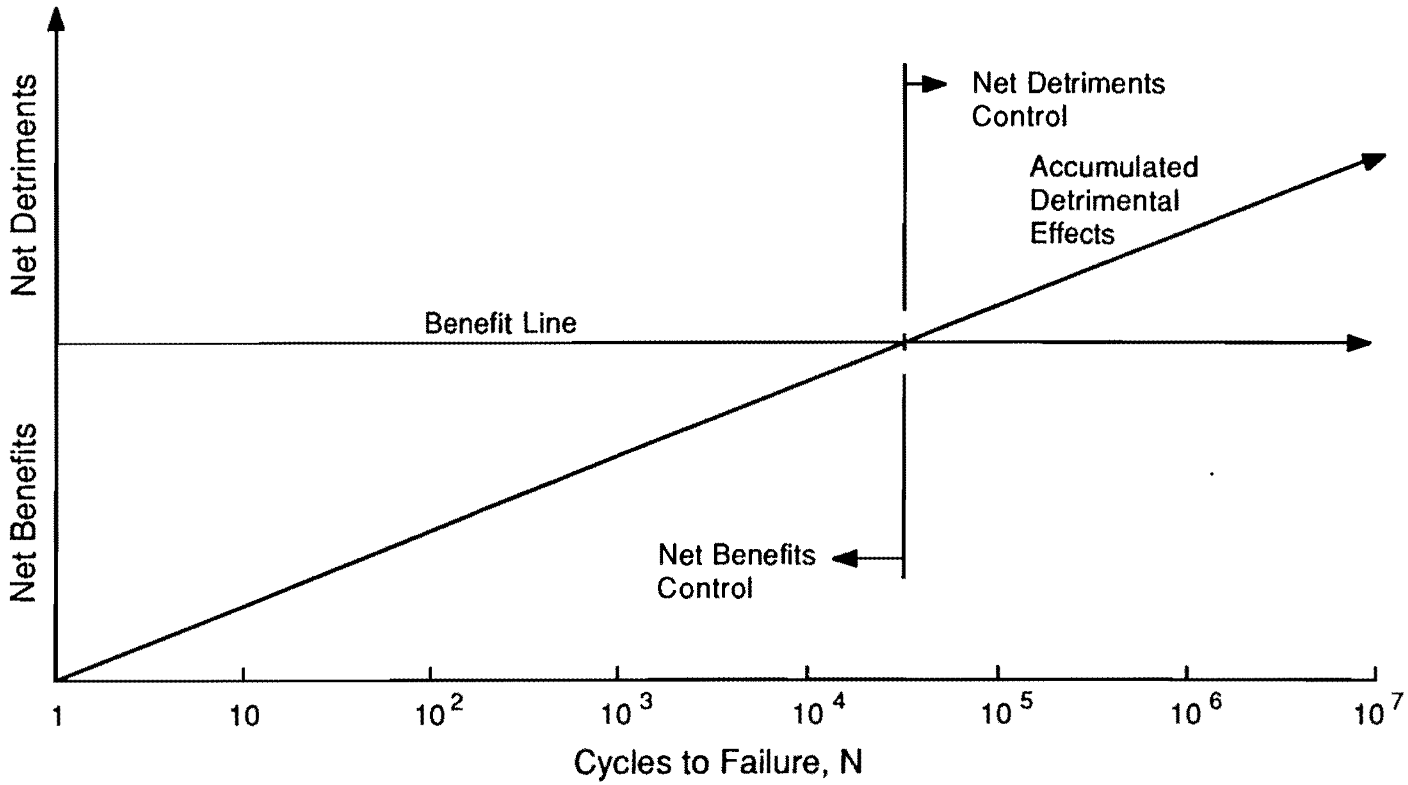

Fig 5.8. Relationship between press benefit and accumulated detrimental effect of higher variation in dynamic stress.

will have a lesser fatigue life than specimens prestressed at 50 psi and tested at the same stress level.

MIDSPAN DEFLECTIONS AND FAILURE MODES

The midspan deflections are presented in Figures 5.9 and 5.10. It can be seen from the graphs that those specimens that were stressed at 150 psi were able to sustain only a few more loading cycles after the first crack before a major crack started propagating across the middepth of the beam. A check of the oscilloscope showed that this was happening despite a drop in the loading. The failure mode was considered as a criterion (3) as defined in Chapter 4, and is shown in Fig 5.11.

However, those specimens that were stressed at 300 psi showed remarkably good elasto-plastic behaviour. When the specimens were reloaded after first crack, the midspan deflection increased considerably at first, but then dropped off. The final deflections were only about one and a half to two times the elastic deflections after a new "equilibrium state" was reached. The curve also shows that, with continued loading, the midspan deflections continue to increase, but not at a very rapid rate. A possible explanation is presented in Fig 5.12.

When the beam was in deflected shape, there was a vertical upward component of the tension force in the prestressing strand which helped to decrease the effect of the applied load. The larger the tension force in the tendon, the larger was the upward component.

In the case of the 150 psi beams, the upward component of the tension force of the prestressing tendon was unable to compensate for the reduced modulus of the concrete beam after the first crack. Therefore, propagation of the crack and the deflection increased rapidly, leading to ultimate failure.

For those specimens stressed at 300 psi, the high prestress tension in the tendons helped to maintain the structural integrity of the beam in an elasto-plastic "equilibrium state". The beams were able to sustain a large number of loadings in this state without the crack propagating above the middepth of the beam. This is shown in Fig 5.13.

These tests were carried out under extreme conditions of no support. For pavements which are supported on a continuous elastic foundation, the amount of prestress required to

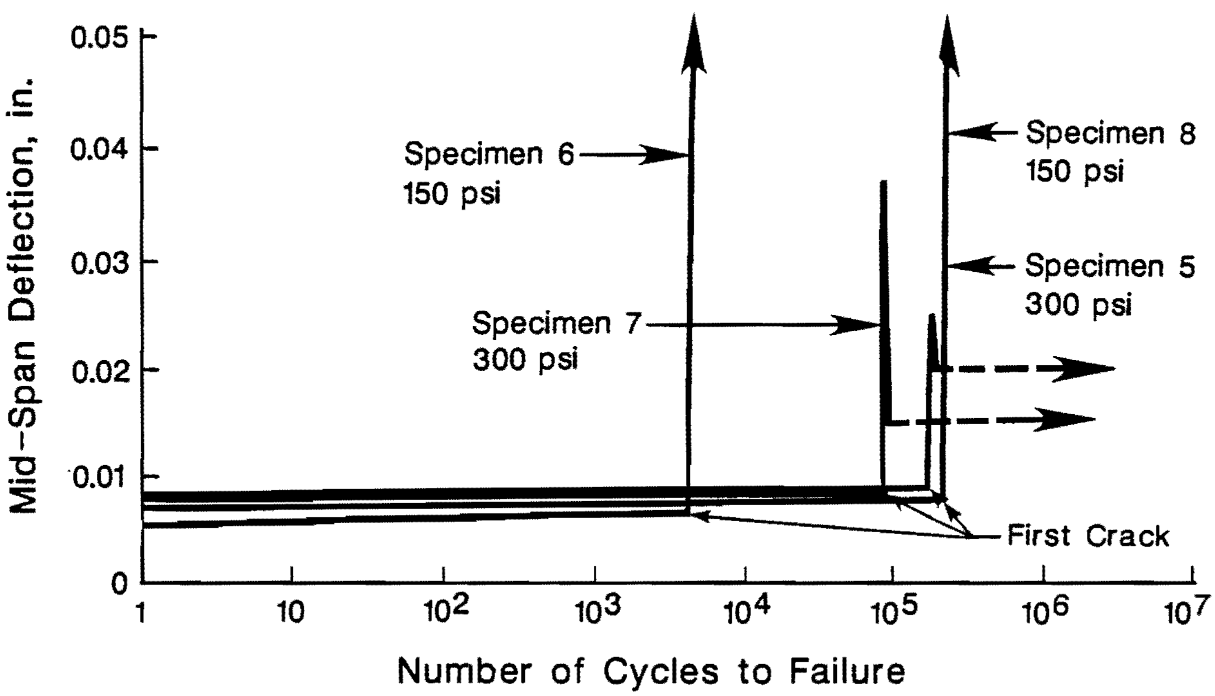

Fig 5.9. Midspan deflection, stress level = 0.7.

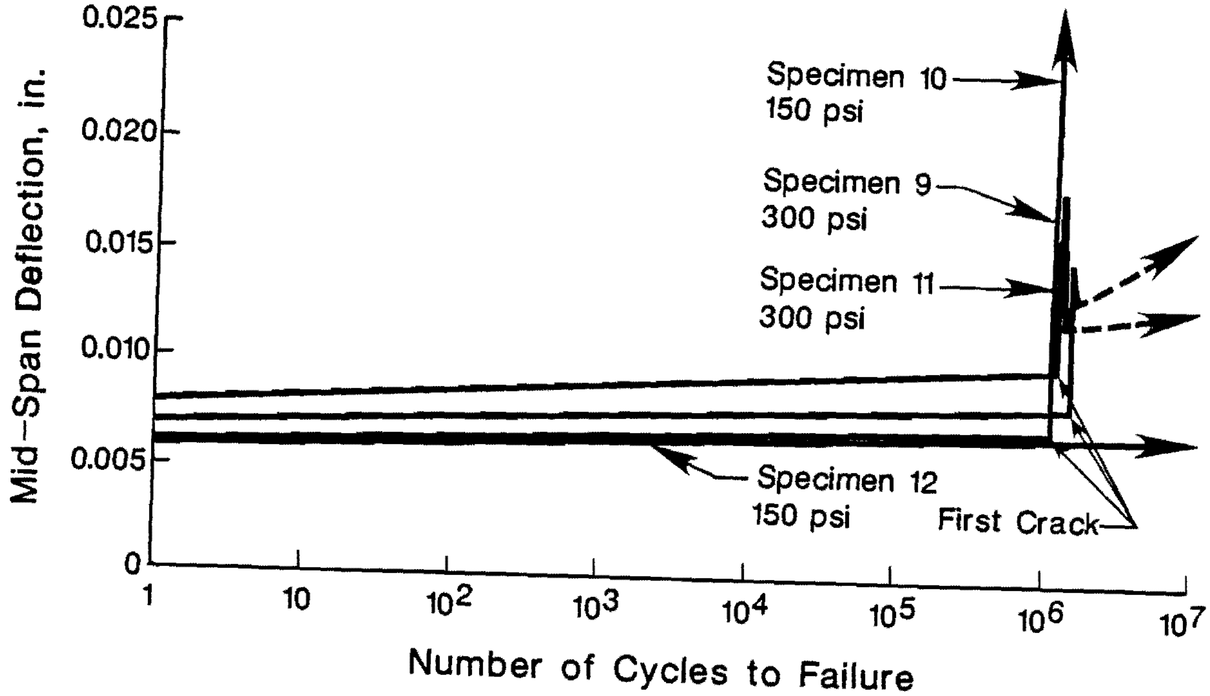

Fig 5.10. Midspan deflection, stress level = 0.60.

(a) Front view.

(b) Bottom view.

Fig 5.11. Failure mode (criterion 3) for 150 psi beams.

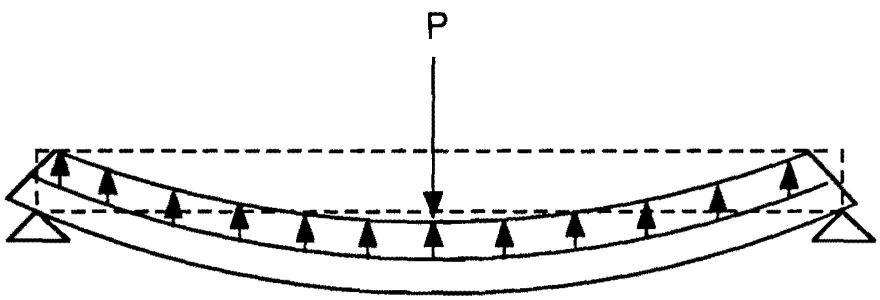

Fig 5.12. Forces in tendon due to the deflected shape of beam.

(a) Front view.

(b) Bottom view.

Fig 5.13. Failure mode (criterion 2) for 300 psi beam.

maintain the structural integrity of the pavements in a elasto-plastic state after cracking may not be so high.

Also, some studies have shown the benefit of moisture at the underside of concrete in the slab. Some compression has been indicated in the bottom fiber in the concrete pavement as a result of this differential moisture effect. These specimens cannot reflect the possible benefit since all their surfaces are exposed to air ventilation on all sides of the beam.

CHAPTER 6. CONCLUSIONS AND RECOMMENDATIONS

The study reported herein was conducted to investigate some underlying assumptions made in the current fatigue design of prestressed concrete pavements. These are the assumptions.

(1) Prestressing does not help in any way to delay microcrack propagation in concrete. Therefore fatigue design is usually based on the fatigue life of plain concrete (Ref 5) or is determined by equations developed from the AASHTO road tests on unreinforced and reinforced concrete pavements (Ref 12).

(2) The resultant stress at the bottom surface of the prestressed concrete pavement can be found by the superposition of stresses. Therefore, the difference between the static nature of prestress and the dynamic nature of the vehicular stresses is not accounted for.

(3) Bottom cracking will result in rapid deterioration of the structural stiffness of the pavement, leading to large increases in deflection and serviceability failure. Therefore, elasto-plastic behavior and the effect of prestress in helping to maintain the structural integrity of the prestressed pavement after bottom cracking are not considered in the design.

In order to determine the validity of these assumptions, the results from fatigue tests of 28 prestressed beams conducted by the Portland Cement Association were evaluated and analyzed. In order to verify the data from the PCA test and to further investigate the effect of prestress on the fatigue life of concrete, a similar investigation was carried out at The University of Texas at Austin. Due to the limited time available, a full scale study was not feasible and only a preliminary investigation was carried out. One of the objectives of this investigation was to identify the important areas of fatigue design in prestressed concrete pavement which need to be further investigated.

CONCLUSIONS

The following summary should not be considered to represent final conclusions as the analysis was carried out on a small sample size, only 40 specimens: 28 specimens from the PCA test program and 12 specimens from The University of Texas at Austin. Another shortcoming is the method by which the modulus of rupture was determined. The S/N relationship is highly dependent on the accuracy by which the modulus of rupture is determined. In the PCA test program, testing of companion specimens may provide unconservative results. At The University of Texas, the modulus of rupture was based on broken halves of failed specimens. Unfortunately, in some cases, only one of the broken halves was available for the static flexure test.

Despite the shortcomings, some salient implications seem to emerge as a result of this investigation.

(1) Prestressing helps to delay the propagation of microcracks in concrete. The higher the level of prestress, the more profound is the effect in delaying the propagation of the microcracks. However, it does not seem that a direct proportional increase is obtained by an increase in prestress level.

(2) The absolute value of the slopes of the equations representing the relationship between stress levels and the logarithm of number of cycles at failure will increase (be steeper) with an increase in the amount of prestress applied.

(3) No fatigue limits exist for prestressed concrete beams subjected to 50 to 300 psi of prestress.

(4) The fatigue strength at 10 million cycles decreases with an increase in the level of prestress. However, all the prestressed beams have a higher fatigue strength than plain concrete. Therefore current fatigue design based on fatigue life of plain concrete is conservative for prestressed pavements subjected to a prestress level of 300 psi or less. Based on the regression analysis results of this investigation, the fatigue strength at 10 million cycles for the 50, 100, 150, and 300 psi specimens are 0.652, 0.583, 0.595 (or 0.587), and 0.560, respectively. While The University of Texas study had a very limited number of samples, making the results less statistically significant, the same

trend of decrease in fatigue strength at 10 million cycles with increase in the level of prestress was observed.

(5) The presumption of superposition of stresses may not be valid because the fatigue life of prestressed concrete is dependent on the interaction of the static nature of prestress and the dynamic nature of the loading stresses. While prestressing provides a constant benefit throughout the life of the concrete, detrimental effects due to dynamic stresses accumulate linearly as the number of cycles of loading increases. In general, when fatigue lives of specimens with two different prestress levels are compared, the specimens with a higher prestress level will have a higher fatigue life if the specimens are subjected to a stress level higher than the stress level at which the two equations intercept. On the other hand, specimens with a lower prestress level will have a higher fatigue life if they are subjected to a stress level lower than the stress level at which the two equations intercept.

(6) The structural integrity of the specimens is highly dependent on the amount of prestress. . Specimens subjected to higher prestress levels were able to maintain better elasto-plastic behavior after the first cracking.

RECOMMENDATIONS

In order to develop a more exact and reliable fatigue design for prestressed concrete pavements, further research in the following areas is recommended. Because of the complexity of the design of prestressed concrete pavements, these recommendations pertain only to the fatigue design aspect.

(1) A full scale study similar to the ones conducted by the PCA and at The University of Texas at Austin should be carried out. In order to more fully appreciate the effect of the prestress, the difference between prestress levels selected should be higher. A good program would be to test specimens prestressed at 50 psi, 200 psi, 350 psi, and 500 psi.

(2) The stress levels at which the equations cross each other should be determined and tabulated. This will provide an easy guide for a designer to choose between

the various prestress levels. As an example, consider the case where the choice of prestress is between 50 psi and 100 psi. It was found earlier (Chapter 5) that the two equations intercepted each other at a stress level of 0.75. If vehicular surveys shows that the pavement to be designed will be subjected mostly to a vehicular stress level less than 0.75, then the smaller prestress will result in longer life.

(3) To better simulate actual pavement conditions, prestressed slabs should be tested on elastic support and with the bottom surface sealed for moisture similar to actual slabs. The effect of longitudinal and transverse prestressing should be investigated.

(4) Tests should be carried out to determine the additional fatigue life after the first crack due to the elasto-plastic behavior of the prestressed concrete.

(5) Further investigations should be carried out to determine the relationship between the static nature of the prestress and the dynamic stresses due to vehicular loadings.

REFERENCES

1. Morris, Gene R., and Hal C. Emery, "The Design and Construction of Arizona's Prestressed Concrete Pavement," Research Section, Highway Division, Arizona Department of Transportation, Fifteenth Paving Conference, University of New Mexico, Department of Civil Engineering, Albuqueque, New Mexico.
2. Hanna, Amir N., Peter J. Nussbaum, Picket Arriyavat, Jim T. Tseng, and Bengt F. Friberg, "Technical Review of Prestressed Pavement," U. S. Department of Transportation, Federal Highway Administration, Offices of Research and Development, Report No. FHWA-RD-77-8, Springfield, Virginia, NTIS, December 1976.
3. Albritton, Gayle E., "Prestressed Concrete Highway Pavement: Construction-As Built Performance, Brookhaven , Mississippi (Research Supplement)," U. S. Department of Transportation, Federal Highway Administration, Region 15, Demonstration Project Division, Arlington, Virginia, August 1978.
4. Gramling, Wade L., T. Paul Teng, Gene R. Morris, and Joe Scheffield, "Prestressed Pavement Performance in Four States, A Panel Report," U. S. Department of Transportation, Federal Highway Administration, Report No. FHWA/RD-82/169.
5. Tayabji, Shiraz D., Bert E. Colley, and Peter J. Nussbaum, "Prestressed Pavement Thickness Design," U. S. Department of Transportation, Federal Highway Administration, Offices of Research and Development, Report No. FHWA-RD, Springfield, Virginia: NTIS, December 1980.
6. Lloyd, John P., James L. Lott, and Clyde E. Kesler, "Fatigue of Concrete," Engineering Experiment Station Builletin No. 499, University of Illinios, Urbana, Illinois, 1968.
7. Sturman, Gerald JM., Surenda P. Shah, and George Winter, "Microcracking and Inelastic Behavior of Concrete," ACI Publication, SP-12, pp 473-499, November 1964.
8. Nagataki, S, and L. Yoneyana, "Studies on Continuously Reinforced Concrete and Prestressed Concrete Pavements Made with Expansive Cement Concrete," ACI Publication, SP-38, pp 313-363, 1973.

9. Nussbaum, Peter J., Shiraz D. Tayabji, and Adrian T. Golks, "Prestressed Pavement Volume 1, Joint Design," U. S. Department of Transportation, Federal Highway Administration, Offices of Research and Development, Report No. FHWA/RD-82/090, Springfield, Virginia, June 1983.

10. O'Brien, J. Scott, Ned H. Burns, and B. Frank McCullough, "Very Early Post-Tensioning of Prestressed Concrete Pavements," Research Report 401-1, Center for Transportation Research, The University of Texas at Austin, June 1985.

11. Cable, Neil O., Ned H. Burns, and B. Frank McCullough, "New Concepts in Prestressed Concrete Pavement," Research Report 401-2, Center for Transportation Research, The University of Texas at Austin, August 1985.

12. Mendoza-Diaz, Alberto, Ned H. Burns, and B. Frank McCullough, "Behavior of Long Presressed Pavement Slabs and Design Methodology," Research Report 401-3, Center for Transportation Research, The University of Texas at Austin, October 1986.

13. Maffei, Joseph R., Ned H. Burns, and B. Frank McCullough, "Instrumentation and Behavior of Prestressed Concrete Pavements," Research Report 401-4, Center for Transportation Research, The University of Texas at Austin, November 1986.

14. Chia, Way-Seng, Ned H. Burns, and B. Frank McCullough, "Field Evaluation of Subbase Friction Characteristics," Research Report 401-5, Center for Transportation Research, The University of Texas at Austin, October 1986.

15. Murdock, J. W., and C. E. Kesler, "Effect of Range of Sress on Fatigue Strength of Plain Concrete Beams," Journal of the American Concrete Institute, Vol 30, No. 2, August 1958, pp 221-233.

16. Clemmer, H. F., "Fatigue of Concrete," Proceedings, American Society for Testing Materials, Vol 22: II (1922), pp 408-418.

17. Hatt, W. K., "Research in Concrete," Purdue University Bulletin No. 24, 1925, pp 44-55.

18. Nordby, Gene M., "Fatigue of Concrete - A Review of Research," Journal of the American Concrete Institute, Vol 30, No. 2, August 1958, pp 191-215.

19. Hilsdorf, H., and Clyde E. Kesler, "The Behavior of Concrete in Flexure Under Varying Repeated Load," TAM Report No. 172, University of Illinois, 1960.

20. McCall, John T., "Probability of Fatigue Failure of Plain Concrete," Journal of the American Concrete Institute, Vol 30, No.2, August 1958, pp 221-233.

21. Hilsdorf, H., and C. E. Kesler, "Fatigue Strength of Concrete Under Varying Flexural Stresses," Proceedings, ACI, Vol 63, October 1966, pp 1059-1075.

22. Ballinger, Craig A., "Effect of Load Variations on the Flexural Fatigue Strength of Plain Concrete," FHWA-RD-72-2, September 1972.

APPENDIX A

RESULTS OF STATIC TESTS ON COMPANION BEAMS, BROKEN HALVES OF FAILED SPECIMENS AND COMPRESSION CYLINDERS

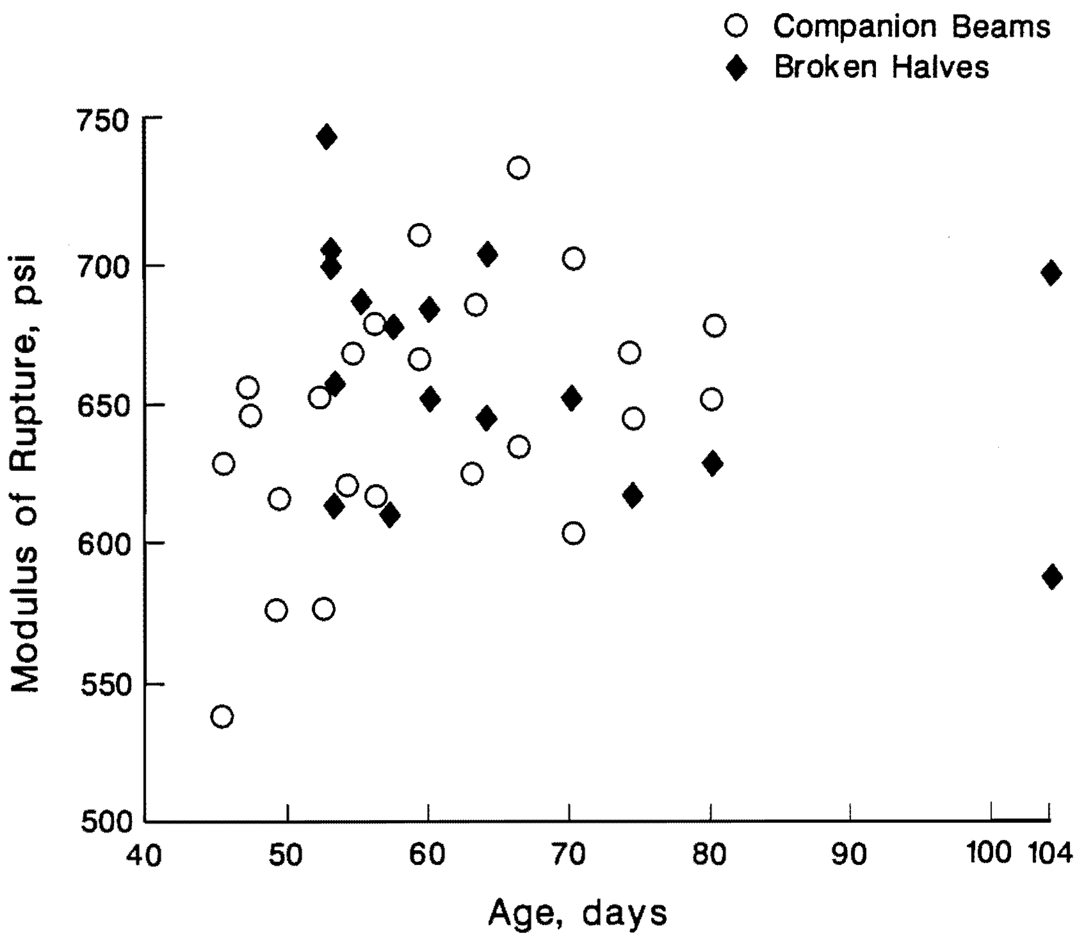

Fig A.1. Flexural strength of companion beams and broken halves.

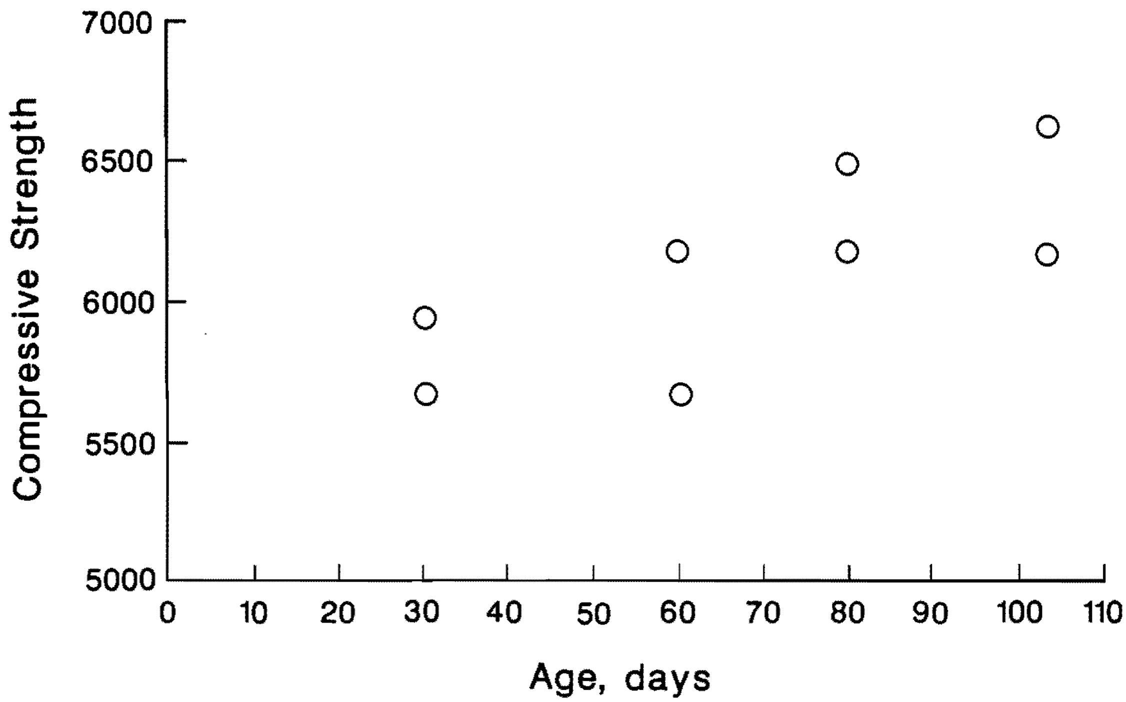

Fig A.2. Compressive strength of concrete cylinders.

TABLE A.1. FLEXURAL STRENGTH OF COMPANION BEAMS

Age (days)	Modulus of Rupture (psi)		
	Beam 1	Beam 2	Average
45	628	538	583
47	646	654	650
49	615	575	595
52	575	651	613
54	620	668	644
56	626	678	652
59	710	666	688
63	683	623	653
66	732	632	682
70	700	602	651
74	666	642	654
80	650	676	663

TABLE A.2. FLEXURAL STRENGTH OF BROKEN HAVLES

Age (days)	Modulus of Rupture (psi)		
	Beam 1	Beam 2	Average
53	698	656	677
53	743	--	743
53	700	--	700
53	613	--	613
55	685	--	685
57	675	609	642
60	650	682	666
64	701	643	672
70	650	--	650
74	618	--	618
80	638	--	638
104	698	652	675

TABLE A.3. COMPRESSIVE STRENGTH OF CYLINDER

Age (days)	Compressive Strength (psi)		
	Cylinder 1	Cylinder 2	Average
30	5920	5672	5796
60	5670	6186	5928
90	6488	6182	6335
104	6309	6614	6462

This page replaces an intentionally blank page in the original.
-- CTR Library Digitization Team

APPENDIX B

REGRESSION ANALYSIS OF FATIGUE TEST DATA

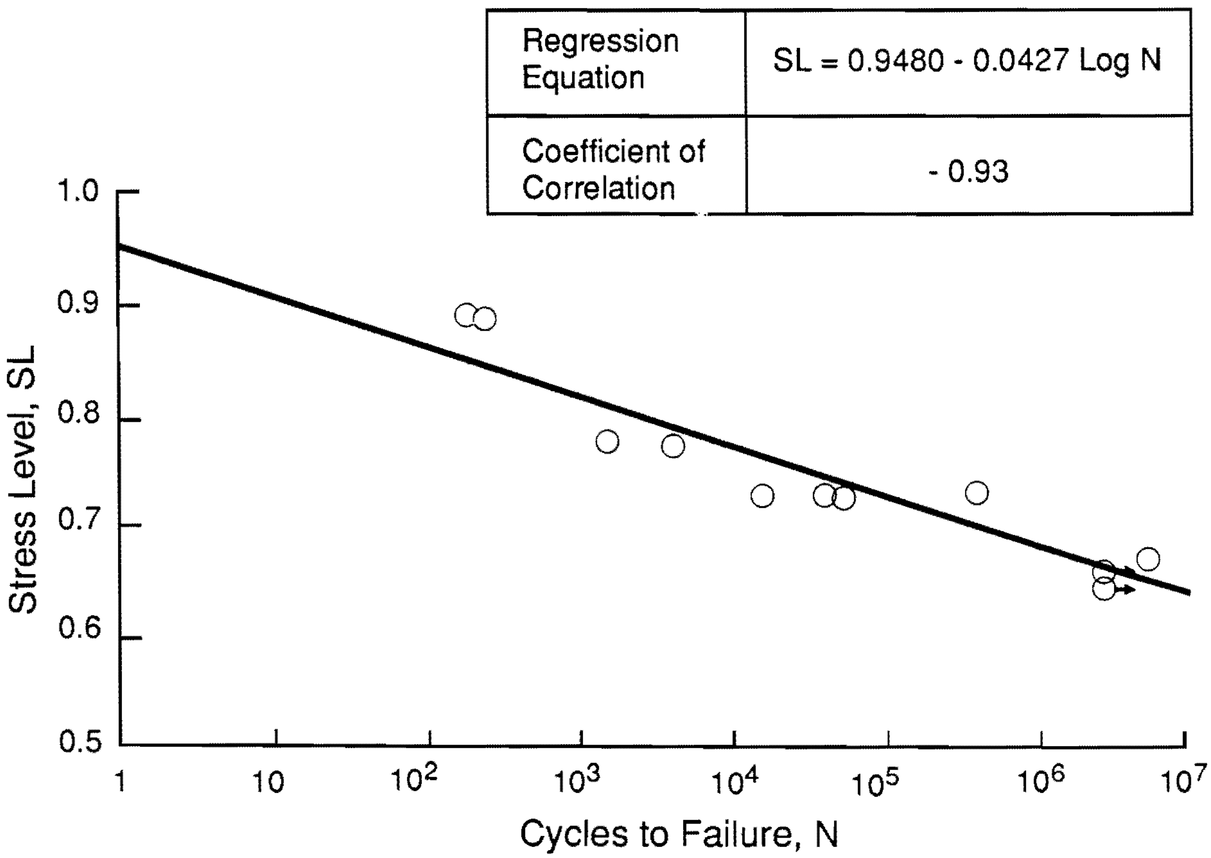

Fig B.1. Regression Analysis 1 (RA1) for beam subjected to prestress level of 50 psi.

Regression Equation	SL = 1.0530 − 0.0654 Log N
Coefficient of Correlation	− 0.92

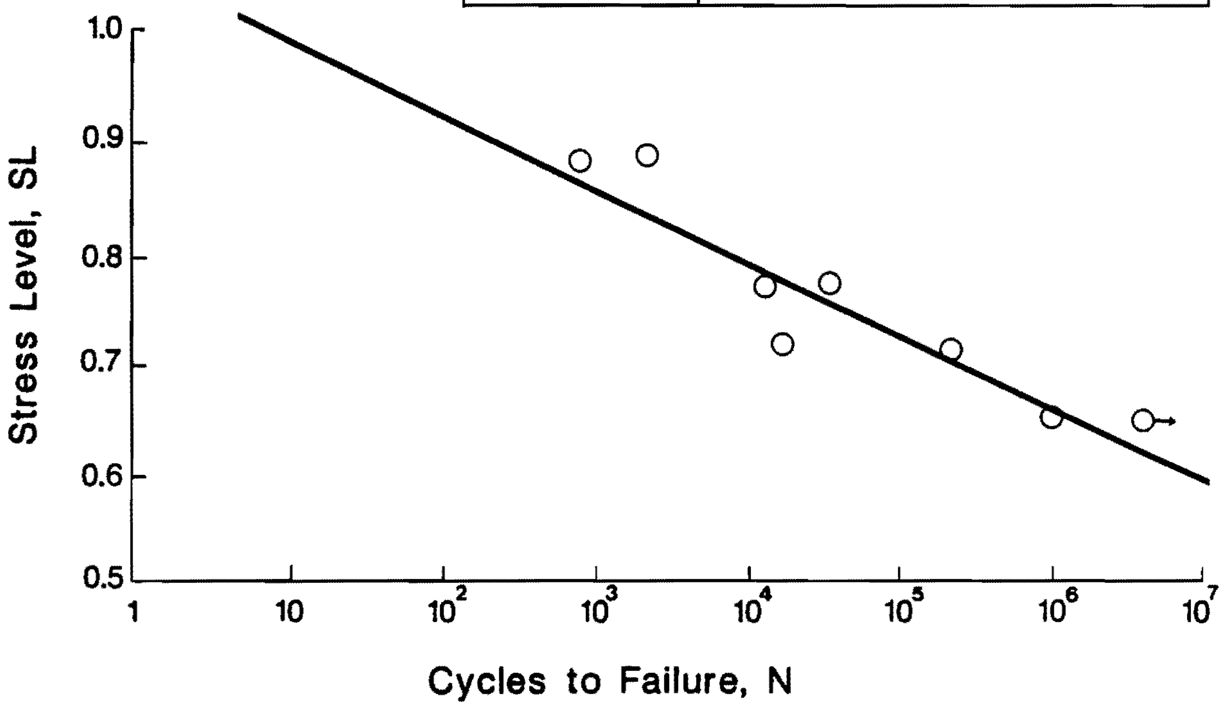

Fig B.2. Regression Analysis 1 (RA1) for beams subjected to prestress level of 100 psi.

Regression Equation	SL = 1.0481 − 0.0650 Log N
Coefficient of Correlation	− 0.88

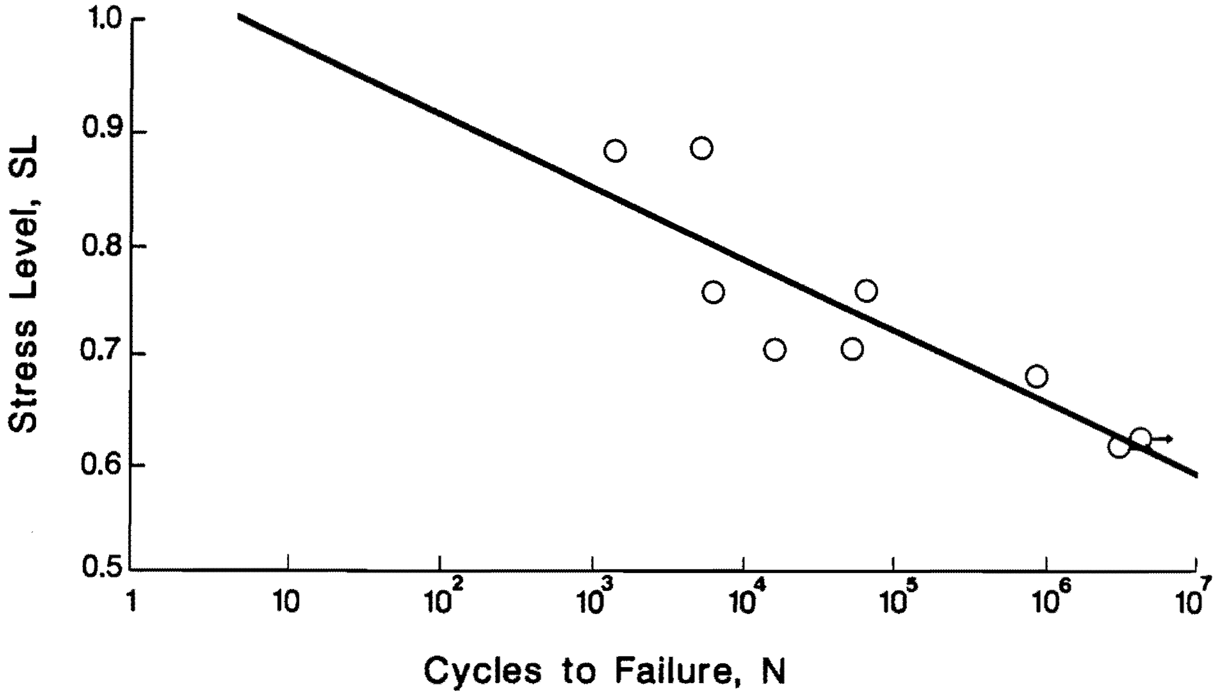

Fig B.3. Regression Analysis 1 (RA1) for beams subjected to prestress level of 150 psi.

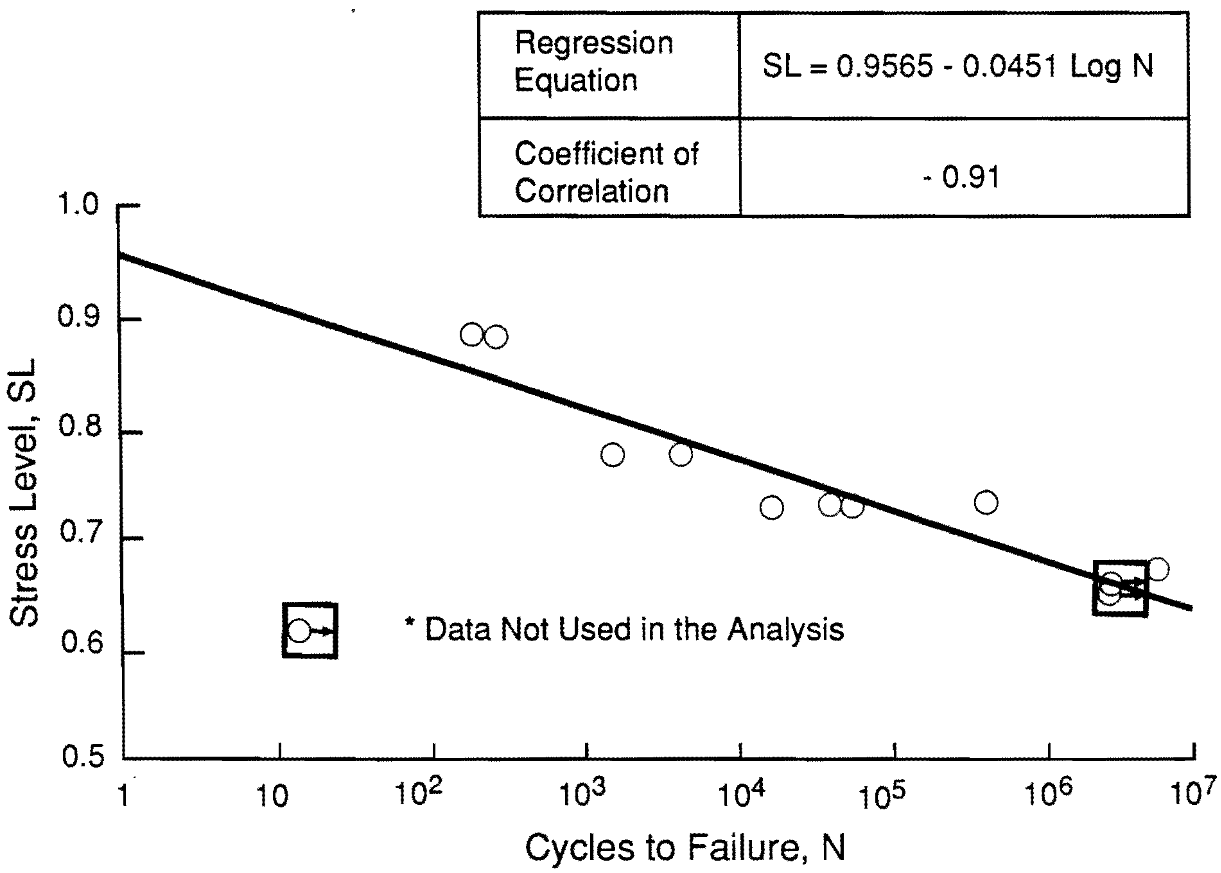

Fig B.4. Regression Analysis 2 (RA2) for beams subjected to prestress level of 50 psi.

Regression Equation	SL = 1.1030 − 0.0781 Log N
Coefficient of Correlation	− 0.93

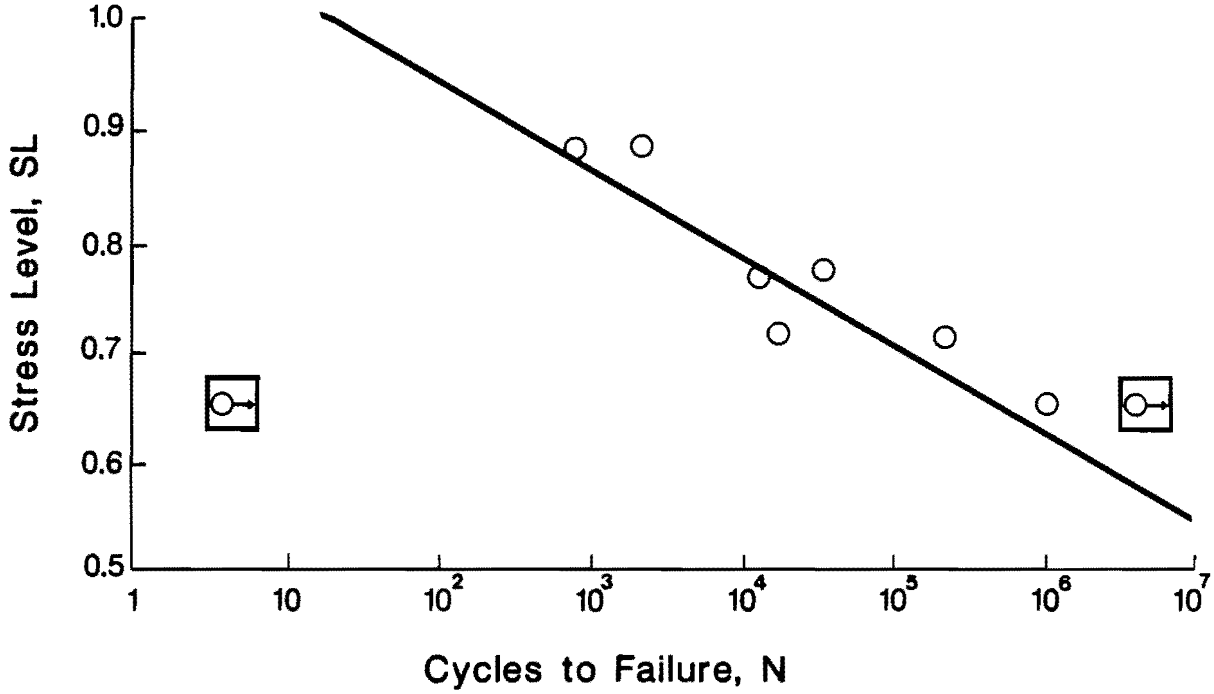

Fig B.5. Regression Analysis 2 (RA2) for beams subjected to prestress level of 100 psi.

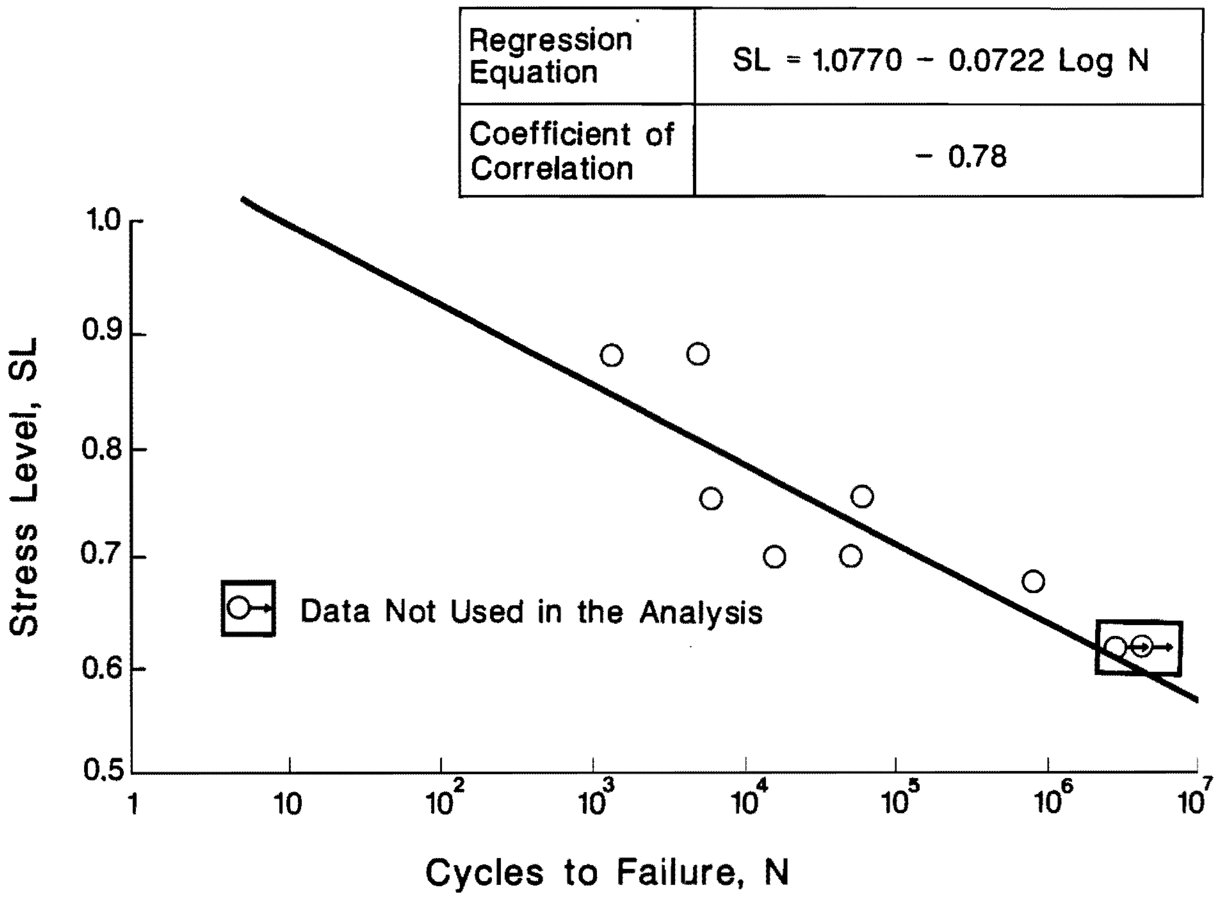

Fig B.6. Regression Analysis 2 (RA2) for beams subjected to prestress level of 150 psi.

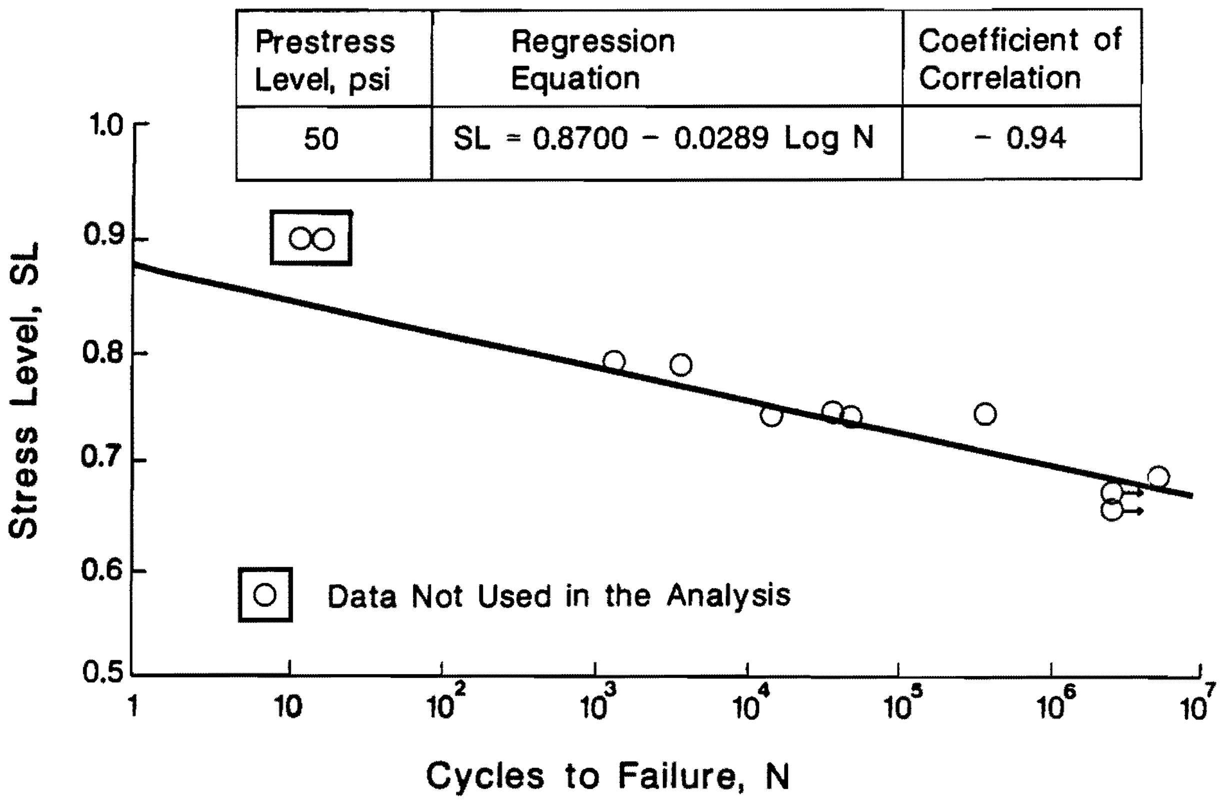

Prestress Level, psi	Regression Equation	Coefficient of Correlation
50	SL = 0.8700 − 0.0289 Log N	− 0.94

Fig B.7. Regression Analysis 3 (RA3) for beams subjected to 50 psi prestress.

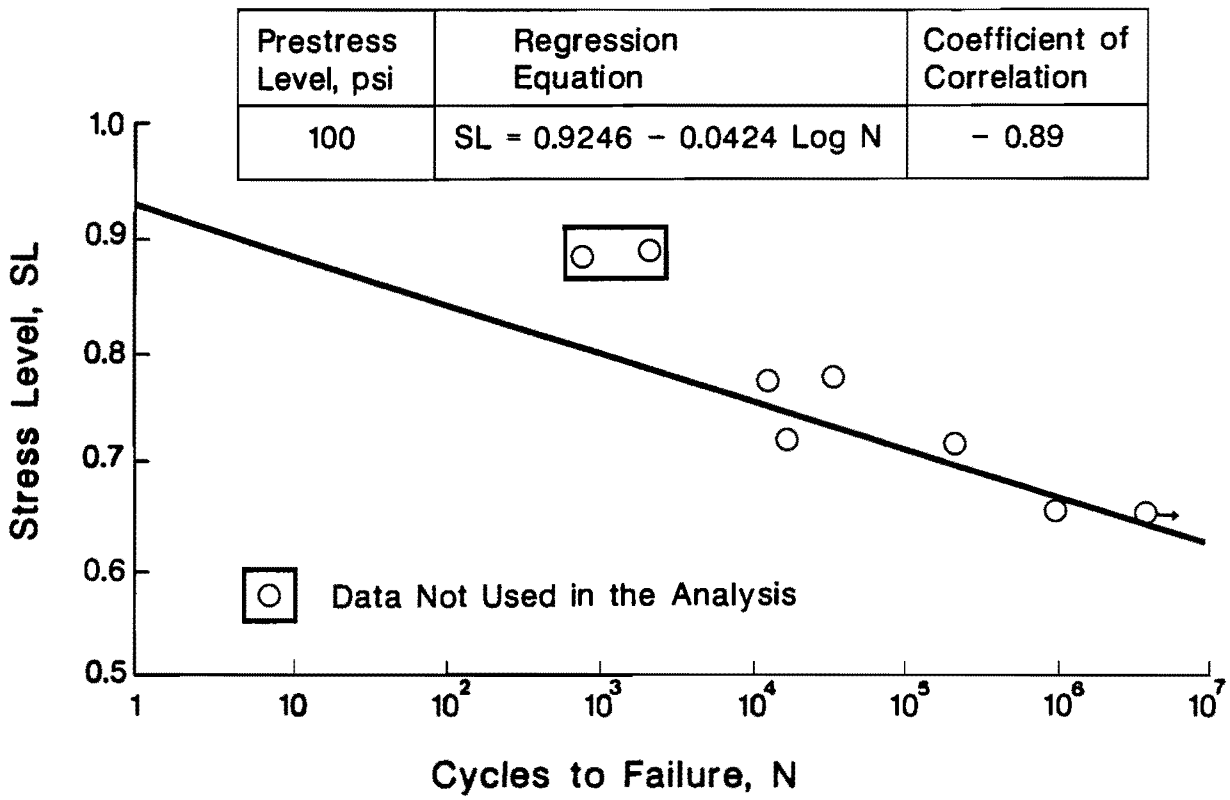

Fig B.8. Regression Analysis 3 (RA3) for beams subjected to 100 psi prestress.

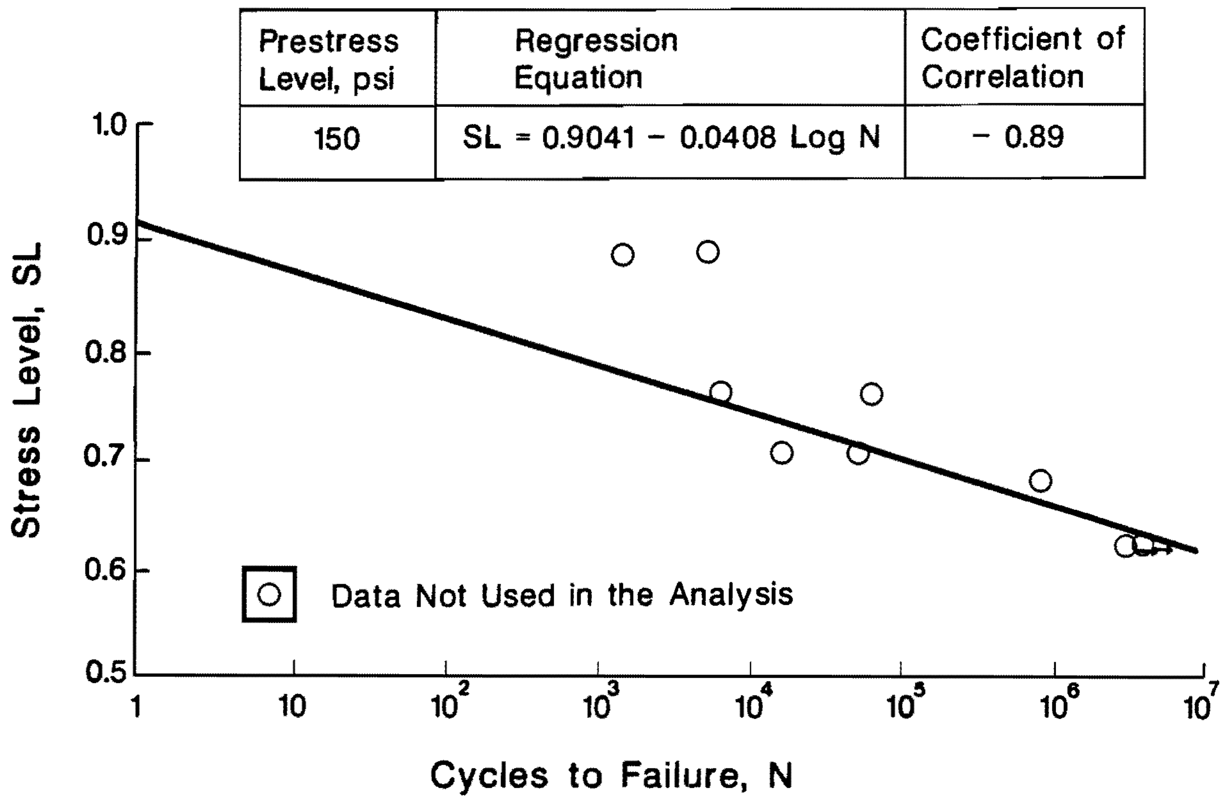

Prestress Level, psi	Regression Equation	Coefficient of Correlation
150	SL = 0.9041 − 0.0408 Log N	− 0.89

Fig B.9. Regression Analysis 3 (RA3) for beams subjected to 150 psi prestress.

TABLE B.1. FATIGUE STRENGTH AT 10 MILLION CYCLES FROM REGRESSION ANALYSIS 1

Prestress Level (psi)	Regression Equation	Fatigue Strength at 10 Million Cycles (F_{10})
50	SL = 0.9480 - 0.0427 Log N	0.649
100	SL = 1.0530 - 0.0654 Log N	0.595
150	SL = 1.0481 - 0.0650 Log N	0.593

TABLE B.2. FATIGUE STRENGTH AT 10 MILLION CYCLES FROM REGRESSION ANALYSIS 2

Prestress Level (psi)	Regression Equation	Fatigue Strength at 10 Million Cycles (F_{10})
50	SL = 0.9565 - 0.0451 Log N	0.641
100	SL = 1.1030 - 0.0781 Log N	0.556
150	SL = 1.0770 - 0.0722 Log N	0.572

TABLE B.3. FATIGUE STRENGTH AT 10 MILLION CYCLES DUE TO REGRESSION ANALYSIS 3

Prestress Level (psi)	Regression Equation	Fatigue Strength at 10 Million Cycles (F_{10})
50	SL = 0.8700 - 0.0289 Log N	0.668
100	SL = 0.9246 - 0.0424 Log N	0.628
150	SL = 0.9041 - 0.0408 Log N	0.619